Title
Effects of biomass burning on summertime nonmethane hydrocarbon concentrations in the Canadian wetlands

Journal
Journal of Geophysical Research, 99(D1)

ISSN
0148-0227

Authors
Blake, DR
Smith, TW
Chen, T-Y
et al.

Publication Date
1994-01-20

DOI
10.1029/93jd02598

JOURNAL OF GEOPHYSICAL RESEARCH, VOL. 99, NO. D1, PAGES 1699–1719, JANUARY 20, 1994

Effects of biomass burning on summertime nonmethane hydrocarbon concentrations in the Canadian wetlands

D. R. Blake, T. W. Smith, Jr., T.-Y. Chen, W. J. Whipple, and F. S. Rowland
Department of Chemistry, University of California, Irvine

Abstract. Approximately 900 whole air samples were collected and assayed for selected C_2-C_{10} hydrocarbons and seven halocarbons during the 5-week Arctic Boundary Layer Expedition (ABLE) 3B conducted in eastern Canadian wetland areas. In more than half of the 46 vertical profiles flown, enhanced nonmethane hydrocarbon (NMHC) concentrations attributable to plumes from Canadian forest fires were observed. Urban plumes, also enhanced in many NMHCs, were separately identified by their high correlation with elevated levels of perchloroethene. Emission factors relative to ethane were determined for 21 hydrocarbons released from Canadian biomass burning. Using these data for ethane, ethyne, propane, *n*-butane, and carbon monoxide enhancements from the literature, global emissions of these four NMHCs were estimated. Because of its very short atmospheric lifetime and its below detection limit background mixing ratio, 1,3-butadiene is an excellent indicator of recent combustion. No statistically significant emissions of nitrous oxide, isoprene, or CFC 12 were observed in the biomass-burning plumes encountered during ABLE 3B. The presence of the short-lived biogenically emitted isoprene at altitudes as high as 3000 m implies that mixing within the planetary boundary layer (PBL) was rapid. Although background levels of the longer-lived NMHCs in this Canadian region increase during the fire season, isoprene still dominated local hydroxyl radical photochemistry within the PBL except in the immediate vicinity of active fires. The average biomass-burning emission ratios for hydrocarbons from an active fire sampled within minutes of combustion were, relative to ethane, ethene, 2.45; ethyne 0.57; propane, 0.25; propene, 0.73; propyne, 0.06; *n*-butane, 0.09; *i*-butane, 0.01; 1-butene, 0.14; *cis*-2-butene, 0.02; *trans*-2-butene, 0.03; *i*-butylene, 0.07; 1,3-butadiene, 0.12; *n*-pentane, 0.05; *i*-pentane, 0.03; 1-pentene, 0.06; *n*-hexane, 0.05; 1-hexene, 0.07; benzene, 0.37; toluene, 0.16.

Introduction

Human activities are altering the trace gas content of the atmosphere on a global scale. The intended burning of biomass and fossil fuels, the destruction of tropical forests, the spread of animal grazing and agriculture into marginal areas, the increasing use of synthetic fertilizers, the release of industrial chemicals into the air and water supply, and urban air pollution are all contributing to worldwide atmospheric change [*Crutzen et al.*, 1979, 1985; *Seiler and Crutzen*, 1980; *Delmas*, 1982; *Iverson*, 1984; *National Academy of Sciences (NAS)*, 1984; *Barrie and Hoff*, 1985; *Greenberg et al.*, 1985; *Ramanathan et al.*, 1985; *Barrie*, 1986; *Crutzen and Andreae*, 1990; *Levine*, 1990; *Lightman et al.*, 1990]. The effects of these emissions already are modifying the Earth's physical condition in the form of acid rain [*Galloway and Likens*, 1981] and stratospheric ozone depletion [*Rowland and Molina*, 1975; *Farman et al.*, 1985].

The yearly amount of biomass burned has increased sharply in the twentieth century [*Levine*, 1990]. During biomass burning, large amounts of carbonaceous material are chemically transformed, volatilized, and injected into the atmosphere. This may occur quickly and violently during the very active stages of fires, or more slowly during the smoldering process. The composition and amount of trace gas production depends upon several factors: the fuel moisture content, the fuel type, the ignition pattern, the terrain, and the meteorological conditions of the region at the time of the burning [*Cofer et al.*, 1988, 1989; *Hegg et al.*, 1990; *Levine*, 1991]. It has been suggested that the burning of biomass is a significant global source of environmentally important atmospheric trace gases, including carbon dioxide (CO_2), carbon monoxide (CO), nitric oxide (NO), nitrous oxide (N_2O), methane (CH_4), and nonmethane hydrocarbons (NMHCs) [*Weiss*, 1981; *Greenberg et al.*, 1984; *Greenberg and Zimmerman*, 1984; *Keeling et al.*, 1984; *Rinsland et al.*, 1985; *Rinsland and Levine*, 1985, 1986; *Andreae et al.*, 1988; *Zimmerman et al.*, 1988; *Cofer et al.*, 1989; *Hegg et al.*, 1990; *Levine*, 1990, 1991; *Jacob et al.*, 1992; *Singh and Zimmerman*, 1992; *Wofsy et al.*, 1992]. The hypothesis has also been advanced that CCl_2F_2 (CFC 12) has been released in globally significant amounts during biomass burning [*Hegg et al.*, 1990].

These trace gases affect tropospheric and stratospheric chemistry and photochemistry. A major part of this photochemistry is controlled through chemical reactions involving HO radicals, the major oxidizing species for many atmospheric trace gases. Despite its importance, measurements of HO concentration have proven elusive in all but a few experiments covering a limited range of atmospheric conditions. Both direct and indirect measurements indicate that

Paper number 93JD02598.
0148-0227/94/93JD-02598$05.00

daytime HO concentrations are in the range of 10^5–10^7 molecules cm^{-3} [*Prinn et al.*, 1992]. These HO reactions control the atmospheric lifetime of the majority of trace gases present in the atmosphere, including NMHCs [*Levy*, 1972; *Logan et al.*, 1981]. Nonmethane hydrocarbons are found in the remote troposphere in mixing ratios ranging from parts per billion by volume (ppbv) (10^{-9}) to less than 1 part per trillion by volume (pptv) (10^{-12}). In regions where NMHCs are at the low end of their concentration range, CO and CH_4 dominate the chemical destruction of the HO radical [*Wofsy*, 1976; *Crutzen and Fishman*, 1977; *Sze*, 1977; *Levine et al.*, 1985; *Greenberg et al.*, 1990; *Singh and Zimmerman*, 1992]. However, in regions with higher NMHC concentrations, such as those encountered routinely in urban locations [*Rudolph et al.*, 1981; *Rasmussen and Khalil*, 1982; *Rasmussen et al.*, 1983; *Tille et al.*, 1985; *Singh et al.*, 1988, 1992; *Blake et al.*, 1992; *Singh and Zimmerman*, 1992] and in biomass-burning events [*Crutzen et al.*, 1979; *Greenberg and Zimmerman*, 1984; *Greenberg et al.*, 1985; *Cofer et al.*, 1988, 1989; *Hegg et al.*, 1990; *Levine*, 1991; *Wofsy et al.*, 1992], the rate of HO radical reaction with the various NMHCs is sufficiently fast to allow them to play a significant role in atmospheric photochemical reaction cycles. The interaction of reactive decomposition fragments from these reactions with nitrogen oxides to form additional ozone is well established [*Stith et al.*, 1981; *Delany et al.*, 1985]. In addition, these fragments can act as carriers of active nitrogen through in situ formation of molecules such as peroxyacetyl nitrate (PAN) [*Singh and Hanst*, 1981; *Aikin et al.*, 1982; *Singh*, 1987; *Singh et al.*, 1992, this issue].

To date, the majority of the large field studies which have quantified emissions of NMHCs from biomass burning have occurred either in the tropics or in the western and southeastern United States [*Crutzen et al.*, 1979; *Seiler and Crutzen*, 1980; *Delmas*, 1982; *Greenberg et al.*, 1984, 1985; *Crutzen et al.*, 1985; *Hegg et al.*, 1990; *Bonsang et al.*, 1991]. Tropical fires have received special emphasis because they are believed to constitute the most significant fraction of atmospheric emissions attributed to biomass burning, particularly during the dry season [*Seiler and Crutzen*, 1980].

Little field research on trace gases emitted during biomass burning has been focused on fires at high latitudes even though this is the location of the world's very extensive boreal forests [*Hegg et al.*, 1990; *Radke et al.*, 1991]. These high-latitude regions, which are believed to be the sites of intense fires, represent more than 10% of the Earth's surface and are projected to be particularly sensitive to the effects of greenhouse warming and global circulation dynamics [*Rahn and McCaffrey*, 1980; *Barrie and Hoff*, 1985; *Cofer et al.*, 1989; *Hansen et al.*, 1989; *Ingram et al.*, 1989]. Furthermore, it has been suggested that specific biological processes may be affected during episodes of reduced stratospheric ozone levels [*Karentz*, 1988]. With this in mind, the Arctic Boundary Layer Expedition (ABLE) 3B project was designed specifically to investigate the atmosphere-biosphere gas exchange processes and to target the sources, sinks, and distributions of CH_4, CO, O_3, PAN, NO_x, NO_y, and specific NMHCs, halocarbons, and organic acids in the Subarctic boreal forest and wetland regions [*Harriss et al.*, this issue].

The focus of this paper is to characterize the extent to which the emissions of trace gases from forest fires and other biomass-burning events encountered during the ABLE 3B project impact the atmospheric chemistry, photochemistry, and climate of this subarctic region. It also addresses the effect of global biomass-burning emissions on the budgets of some of the longer-lived NMHCs.

Experiment

The Arctic Boundary Layer Experiment 3B was conducted in July and August 1990 in central and northeastern Canada, with the NASA Electra playing a central role as an experimental platform. During the 5-week intensive aircraft campaign of this project, 883 discrete air samples were collected in individual air canisters on board the Electra and assayed for selected halocarbons and NMHCs [*Smith*, 1993]. A temporary laboratory was established for 3 months at Canadore College, North Bay, Ontario, Canada, for the purpose of assaying the collected samples as rapidly as possible. In this manner, most of the available 300 air sampling canisters were filled approximately 3 times during the project.

Preparation of Stainless Steel Canisters

Previous research in our laboratory and in several others has shown that successful containment of some halocarbons and hydrocarbons is strongly affected by the nature of the inner surfaces of the containment vessel and by the cleaning processes used for these surfaces. Therefore we are providing here a detailed description of the cleaning processes used during the construction of our stainless steel canisters. Each canister was constructed from a commercially available 2-L stainless steel beaker which had been trimmed at the top and fitted with a lid and a single NUPRO SS-4BG-STHT bellows valve. These valves were rinsed 4 times each with acetone (note that all acetone used in the cleaning process was of nanograde purity) placed in a tray containing acetone and ultrasonically cleaned for 20 min. After air drying for at least 12 hours, the valves were baked in ambient air in the following sequence: 6 hours at 80°C; 3 hours at 130°C, and 12–15 hours at 225°C.

The stainless steel beakers were purchased from the Baker Chemical Company, and the lips were removed by the Ebtec Company. The beakers then were scrubbed briskly in mild detergent for about 2 min, rinsed, and allowed to sit full of distilled water for 20 to 60 min. Next, the beakers were rinsed with acetone, then ultrasonicated for 20 min in another bath of acetone, rinsed again with acetone, and then air dried.

The can lids and holes for the valve connectors were cut by electron beam and then a port connector was electron-beam welded to the lid. The lids were washed in a mild detergent and a cotton swab was pulled through the port connector to remove any residue inside. The lids, which sat for about an hour in distilled water, first were rinsed with acetone, then ultrasonicated in acetone for 20 min, rerinsed with acetone, and air dried. After cleaning, the canisters were stored in plastic bags and then transported to the welding site. The lids were electron-beam welded onto the cans and all welds were helium-leak tested. After transport to the home laboratory, valves were swaged onto the port connectors making a complete canister. The canisters were vacuum baked (10^{-5} torr) using the previously given temperature/time sequence. After flushing the baked cans 3 times with ambient air, the canisters were put immediately to

use in the NASA ABLE 3A experiment conducted in Alaska [*Blake et al.*, 1992]. On first use, these canisters were quite satisfactory for alkanes, acetylene, and several halocarbons, but the light olefin concentrations tended to grow with time during repetitive measurements of successive aliquots from individual canisters. After the ABLE 3A experiments and prior to ABLE 3B the canisters were filled with ambient air and baked with the valves open following the temperature and time sequence previously mentioned. The alkene stability problems were solved by this ambient air baking.

Canister sample integrity studies included repetitive measurements of individual samples from the aircraft. Because the time delay between collection and analysis was always in the hours to days range for aircraft samples, a separate test of integrity was made on a ground level sample. Air from the pine woods immediately outside the Canadore laboratory was introduced at ambient pressure into an evacuated 2-L canister. Within 2 minutes a 250-ml (STP) sample was preconcentrated on the glass bead loop and injected onto the separation columns. This sample was assayed subsequently 1 hour, 24 hours and 3 weeks later. No significant deviations ($\pm 1\sigma$) in any of the mixing ratios of the reported NMHCs and halocarbons were observed. These studies confirm that the canisters maintained sample integrity for at least several weeks. No direct information is available about possible alterations in trace gas concentrations occurring in the canisters during the 2 min between collection and analysis, but the consistency of the results suggests any such concentration variations to be negligible. The stability in these canisters of C_2H_4, C_3H_6, and C_5H_8, all of which have significant reactivity with O_3, suggests that ambient O_3 is removed by the metal surfaces of the canister almost immediately after collection, without involving the olefins present in much smaller quantities. These results are consistent with those reported previously [*Greenberg et al.*, 1992].

Sample Filling Procedure

Outside air was brought into the NASA Electra through a 1/2-inch stainless steel air intake mounted on the port side of the fuselage, forward of the wing section, and extending out 8 inches, beyond the boundary layer of the Electra. The inlet was attached to a two-stage metal bellows pump (Metal Bellows Company, MB-602) connected in series allowing for pressurization to 40 (psig). The canisters were configured in three columns of eight each via 1/4-inch stainless steel ultratorr tees equipped with VITON O rings and 1/4-inch stainless steel tubing. These 24-canister "snakes" formed the basic unit for handling operations on the NASA Electra and for air shipments when the Electra was not based at the North Bay airport, adjacent to the Canadore laboratory. A gas-handling manifold mounted on top of the rack directed the airflow to any one of the three 24-canister snakes connected in parallel. The exhaust line was mounted above the top of the fuselage. Once the Electra was airborne, the 200-ml manifold and snake were flushed with several hundred liters of ambient air prior to filling the first canister. This procedure adequately expelled any cabin air which had been incorporated in the lines during the installation of canister sets prior to the commencement of the mission. The time required to pressurize a sample to 40 psig ranged from 10 to 60 s depending on the ambient pressure associated with a particular altitude. Therefore depending on the speed and/or ascent/descent rate of the Electra, each sample represents an air mass collected over a linear distance of several kilometers or a vertical distance of as much as 150 m.

Prior to the beginning of the aircraft missions, pump integrity and contamination studies using humidified zero air were performed on the entire manifold system. The zero air was passed through the inlet, pump, and manifold before collection in the canister, exactly as ambient samples were collected on the Electra in flight. Test results showed no increase in any mixing ratios of reported NMHC and halocarbons. Additionally, pressure dependent studies were performed to simulate pump performance at different altitudes, and the results again showed no significant deviations in mixing ratios of the measured trace gases.

Samples were usually analyzed within 4 days and always within 7 days of collection. Some of the delay in analysis resulted from the necessity for shipping of air canisters via commercial air cargo from the Electra area of operation to the Canadore laboratory. The logistics for the simultaneous arrival of 72 newly filled canisters inevitably caused as much as a 30-hour delay in analysis for the last few canisters in a shipment. Once the samples were assayed, the canisters were evacuated to a pressure of 10^{-2} torr and shipped back to the Electra for subsequent use.

Chemical Analysis

Each air sample was analyzed for NMHCs and halocarbons utilizing a trace gas analytical system composed of three separate gas chromatographic columns enclosed in two independently programmed temperature-controlled GC ovens (see Figure 1). Two of the columns were equipped with flame ionization detectors (FID) and the third with an electron capture detector (ECD). Approximately 650 torr of air was transferred from the canister to a 2-L stainless steel storage vessel permanently fixed to the vacuum line. The less volatile trace gases were preconcentrated on a loop (24 inches × 1/8-inch OD stainless steel) filled with 1-mm-diameter glass beads and immersed in liquid nitrogen. This procedure allowed the separation of the trace gases from the bulk N_2, O_2, and Ar but did not quantitatively trap CH_4. After 500 torr of sample in the storage vessel plus line (1275 cm^3 at STP) had passed through the preconcentration trap, the loop and its contents were isolated via an 1/8 inch UWP six-port switching valve with 0.03-inch orifices (Valco Instruments) and heated with hot water (40°–60°C) to revolatilize the trace gases. The H_2 carrier was redirected to flush the previously trapped contents from the loop to the splitter box which partitioned the gas flow to the three different columns. The 1/16-inch SS tubing from the switching valve to the splitter box was connected to a 1/16-inch SS cross. Different lengths of 0.25-mm deactivated fused silica were connected to the cross. The length depended upon how much restriction was necessary to yield the desired flows to each column. The precision obtained during this study indicated that the partitioning of flows was extremely reproducible. Forty-five percent of the flow was directed onto a 50-m 0.32-mm Al_2O_3 plot column (Chrompak), 30% to a 60-m 0.53-mm DB-1 column (J & W Scientific) and 25% to a 75-m 0.53-mm DB-624 column (J & W Scientific). The plot column, used for C_2-C_7 analysis, was attached to one of the FIDs in GC 1 and the DB-1 column, used for C_4-C_{10} separations, was plumbed into the second FID of GC 1. The DB-624 column in GC 2 was attached to an ECD and was used to characterize the C_1-C_2 CFCs and several halocar-

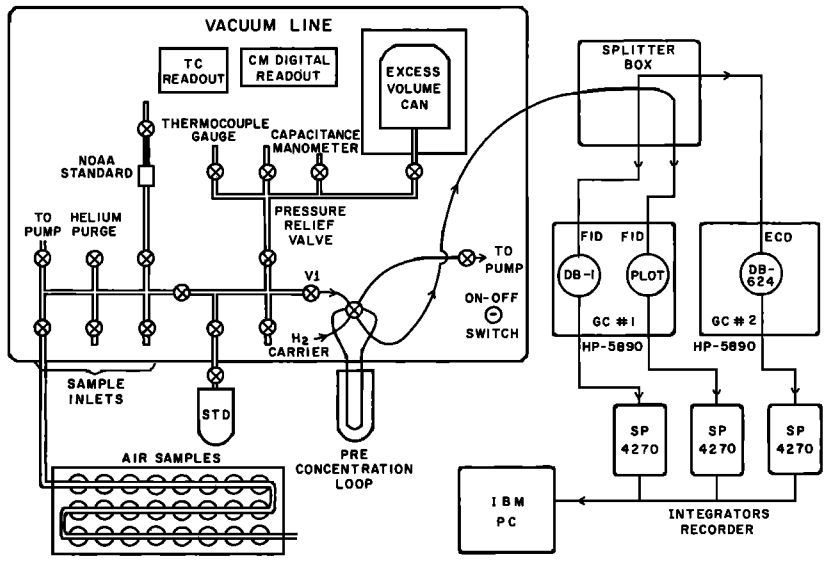

Figure 1. Nonmethane hydrocarbon (NMHC) and halocarbon trace gas analytical system.

bons. The temperature program of GC 1 was 35°C for 5 min, then ramped at 20°C min^{-1} to 130°C, then to 190°C at 10° min^{-1}, held for 6.5 min at 190°C, and terminated. The temperature program of GC 2 had an initial temperature of 35°C for 8 min, was ramped to 260°C at a rate of 30°C min^{-1}, held for 4.5 min at 260°C, and terminated. The time required for one complete cycle of trapping and injecting a sample was about 27 min. Continuous operation of the gas chromatographic apparatus (24 hours a day, 7 days a week for 6 weeks) allowed for the analysis of approximately 50 ambient samples and/or standards per 24-hour period. Because a whole air standard was used during the entire project, fractionation and split ratio differences between standards and samples was not an issue.

The three chromatograms of a typical background sample unaffected by recent urban or biomass-burning plumes collected at a median altitude of 1320 m during mission 4 are shown in Figures 2–4. The sections of the chromatograms between 7 and 15 min from the plot column of this 1320-m sample and from another sample collected 4 min later in a fire plume encountered at 1970 m are displayed in Figures 5 and 6. Although a substantial number of gases elute during this time, peak separation is generally quite satisfactory. Because no backflushing was employed with any of the

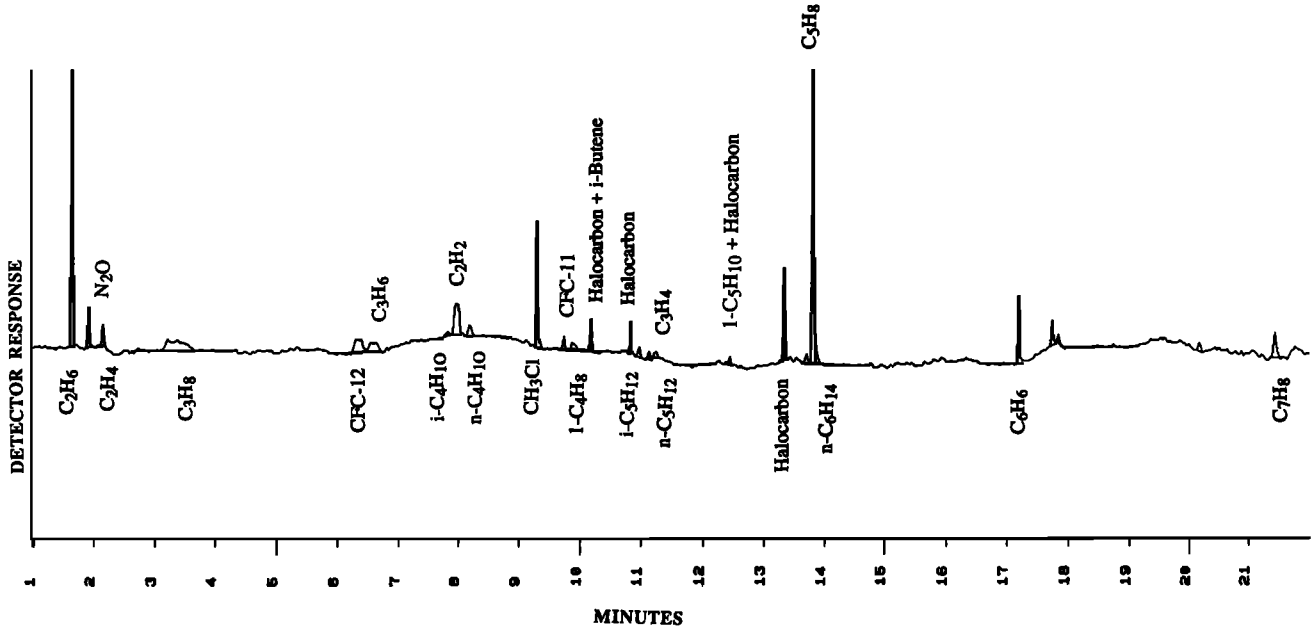

Figure 2. An example chromatogram from the 50-m 0.32-mm Al_2O_3 plot column representing background ambient air collected at 1320 m altitude during the vertical profile on mission 4 and used in the determination of C_2-C_7 NMHC mixing ratios.

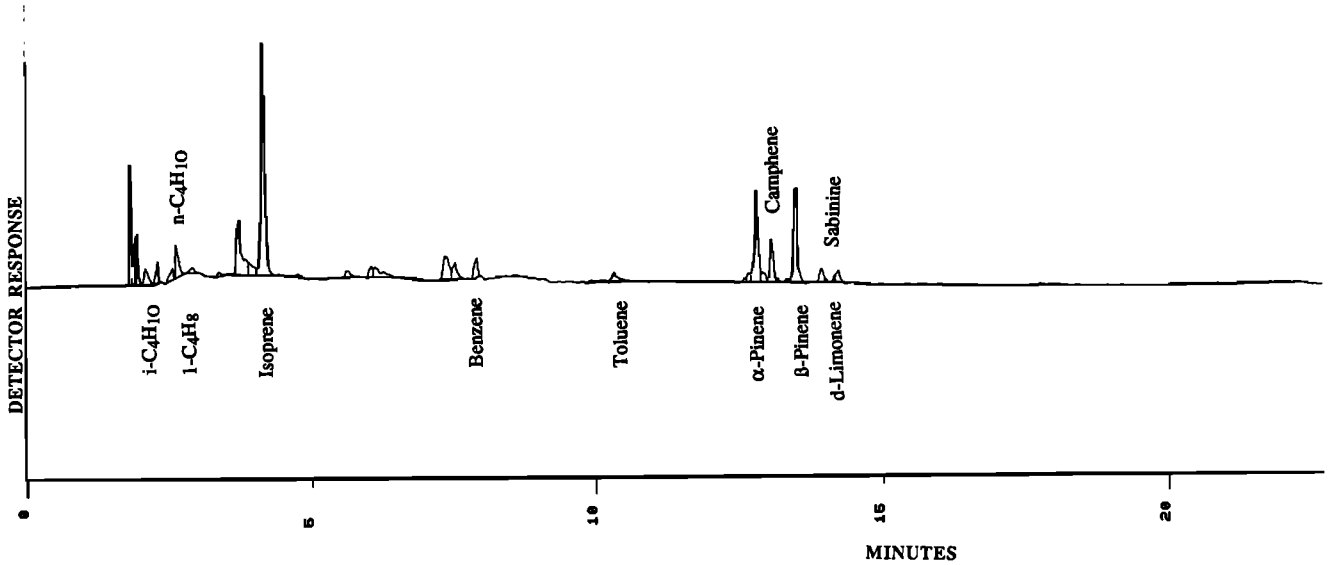

Figure 3. An example chromatogram from the 60-m 0.53-mm DB-1 column representing background ambient air collected at 1320 m altitude during the vertical profile on mission 4 and used in the determination of C_4-C_{10} NMHC mixing ratios.

columns, late emerging peaks on the plot column from one sample sometimes came out as a perturbed broad background in subsequent analyses.

The trace gas analytical system was interfaced to three Spectra Physics Chromjet computing integrators and an IBM PS2 computer for data acquisition, storage, and reduction. While the data output direct from the integrators was sufficiently useful for preliminary data, the occasional variations in baseline behavior and retention times required subsequent visual confirmation of compound identification and baseline assignment for each peak in every chromatogram.

A secondary standard, provided in early 1990 by NOAA scientist Paul Steele (now at CSIRO in Australia) was used throughout the ABLE 3B project as the working standard. It was a partially dried (3 parts per million by volume (ppmv) H_2O) whole air sample collected at Niwot Ridge, Colorado, and contained in an Aculife-treated Luxfur cylinder pressurized to 2000 psig. It was assayed between each set of 12 canisters in the same manner and procedure used to analyze the samples. Repetitive comparisons with several gas mixtures employed as reference standards demonstrated that the concentrations of gases in the working standard exhibited no statistically significant changes in their mixing ratios during 190 measurements over the course of the ABLE 3B project. All halocarbons and NMHCs described in this paper except 1,3-butadiene, *trans*-2-butene, and *cis*-2-butene were present

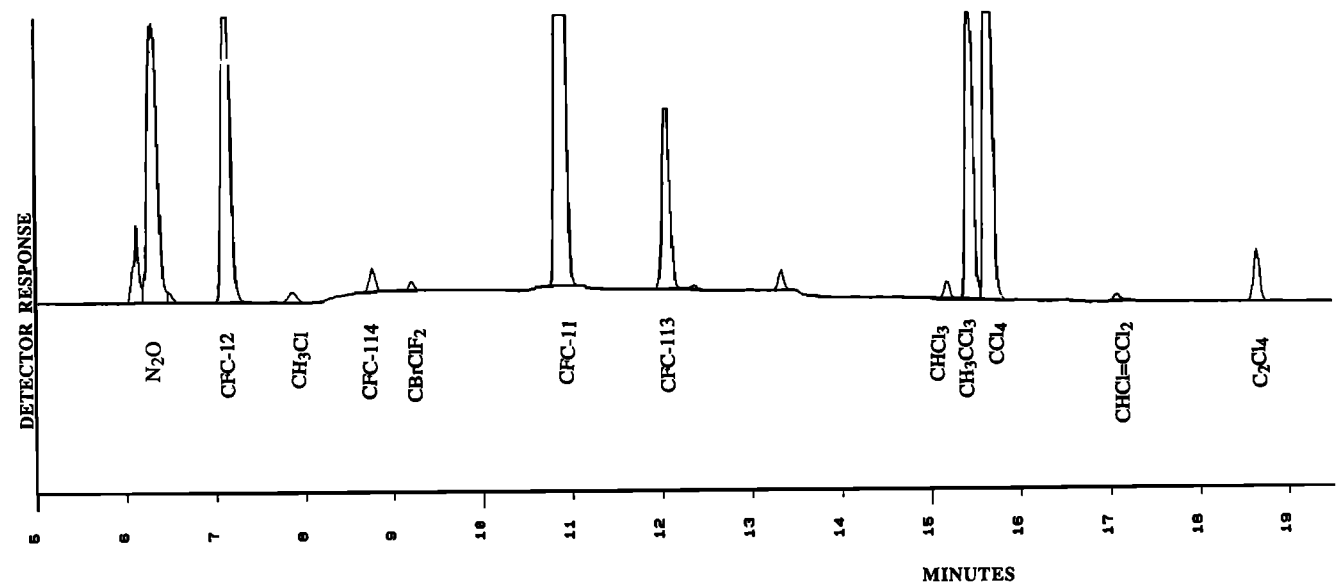

Figure 4. An example chromatogram from the 75-m 0.53-mm DB-624 column representing background ambient air collected at 1320 m altitude during the vertical profile on mission 4 and used in the determination of C_1-C_2 CFCs and selected halocarbon mixing ratios. The peaks for CCl_2F_2, CCl_3F, and CCl_4 are all off scale and truncated in this diagram.

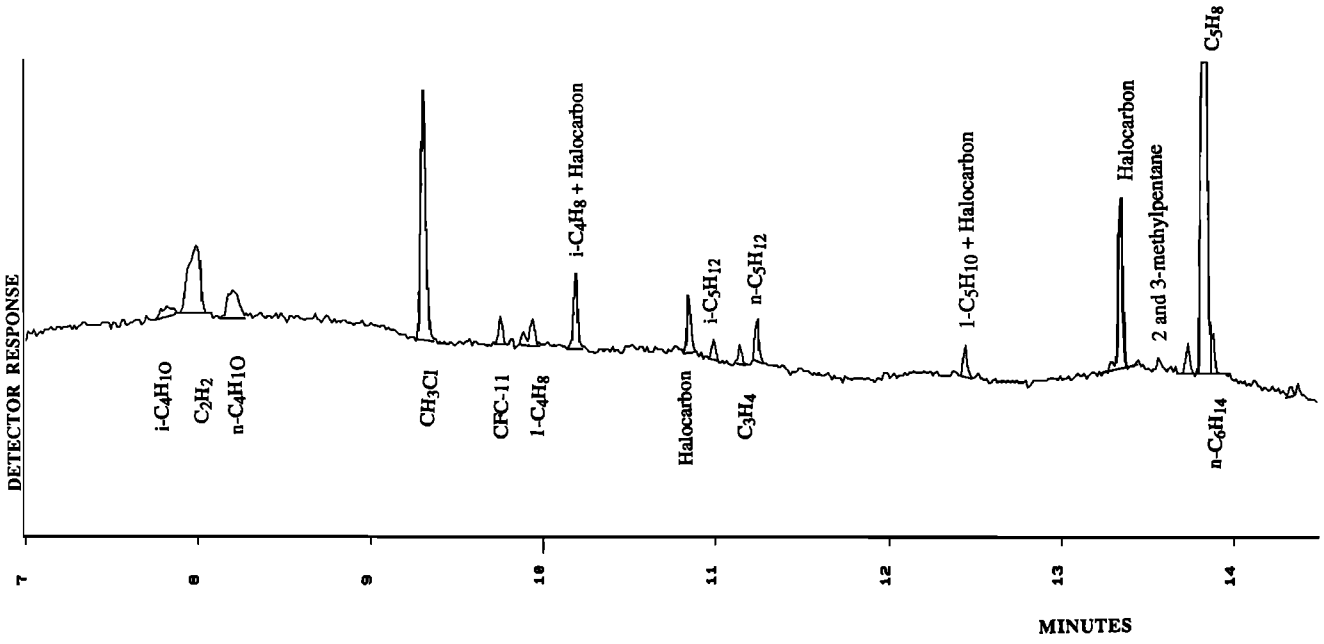

Figure 5. The same plot column chromatogram as in Figure 2 except expanded in the 7- to 15-min region to characterize the reactive C_4-C_6 NMHCs.

in detectable amounts in the working standard. Nonmethane hydrocarbon reference standards with a stated accuracy of 2% (95% confidence limit) were obtained from Scott Specialty Gases (Plumsteadville, Pennsylvania). The mixing ratio of propane in the Scott standard was confirmed by comparison to a methane-propane mixture provided by the National Bureau of Standards (SRM 1660A) which had a stated accuracy of 1% (95% confidence limit). The accuracy of the NMHC calibration procedure after dilution down to the low ppbv/high pptv range is estimated to be 5%. The halocarbon calibration gases were prepared on the same analytical systems as reported by *Tyler* [1983], *Gilpin* [1991], and *Wang* [1993] with an absolute accuracy for the various gases in the 2–10% range.

Specific peaks detected by the FIDs were identified by comparison to the various Scott calibration standards, which contain four to nine gases, and to qualitative standards prepared at our home laboratory, each containing one gas diluted in helium. Because of the sensitivity in elution times of the plot column to variations in trace concentrations of H_2O and CO_2, the column was subjected during the peak identification procedure to the same chemical conditions as

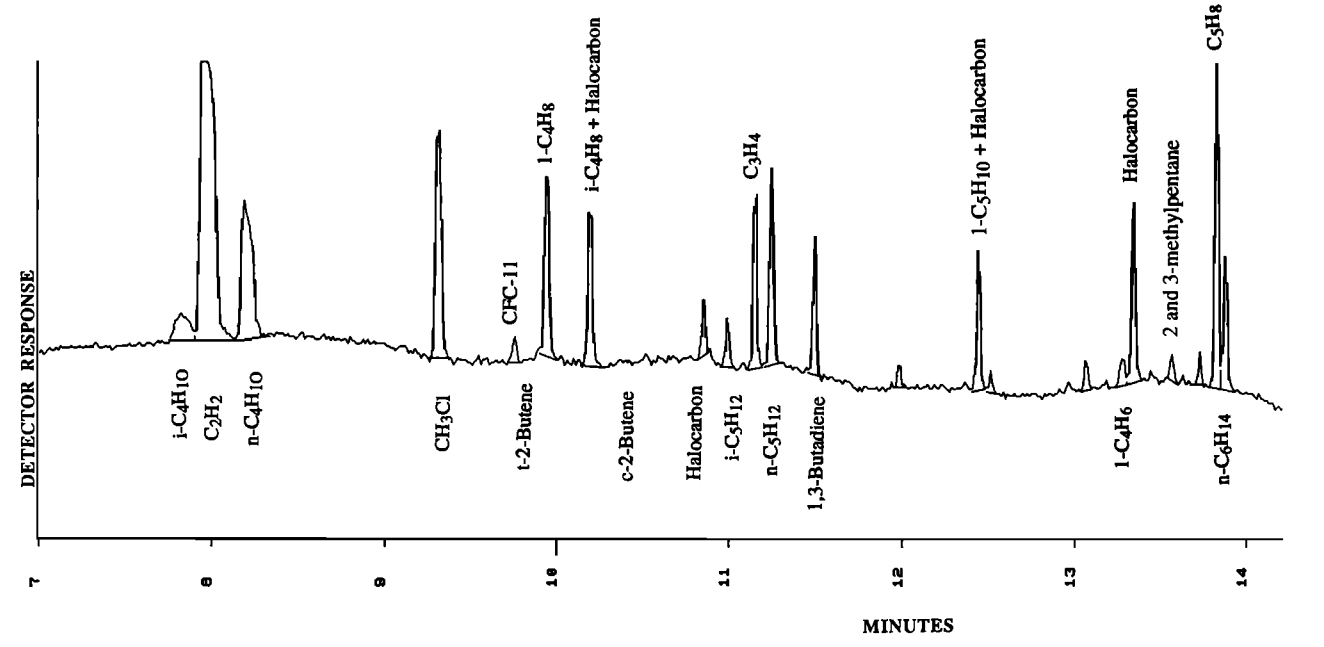

Figure 6. An example chromatogram from the plot column expanded in the 7- to 15-min region representing the elevated emissions of the reactive C_4-C_6 NMHCs in a biomass-burning plume encountered at 1970 m altitude during the vertical profile on mission 4.

Table 1a. Hydrocarbon Mixing Ratios (pptv) for Spiral Descent at 51.5°N, 81.8°W, July 17, 1990, ABLE 3B, Mission 4

Altitude, m	Ethane	Ethene	Ethyne	Propane	Propene	Propyne	*n*-Butane	*i*-Butane	*n*-Pentane	*i*-Pentane	*n*-Hexane	Benzene	Toluene	Isoprene
5350	813	73	125	120	0	4.1	28	9.0	8.1	6.2	2.5	55	18	0
5200	773	54	111	115	0	3.1	26	9.6	6.9	5.3	2.5	47	10	0
5060	717	44	81	88	0	0.0	21	8.9	5.5	4.3	0.0	42	14	0
4900	773	64	111	93	11	3.1	25	8.5	6.3	4.5	2.5	44	12	0
4770	719	41	93	68	34	3.3	14	8.0	3.8	3.7	0.0	45	16	0
4630	738	47	92	64	0	2.1	17	8.1	4.3	2.4	2.4	35	7	0
4520	765	61	104	73	0	2.6	17	8.2	5.2	3.1	2.0	45	10	0
4380	761	71	107	80	15	3.2	22	8.9	5.7	3.4	2.4	47	8	0
4240	727	62	95	67	0	2.9	20	7.4	4.7	2.9	2.3	42	7	0
4120	681	35	76	40	0	3.0	11	7.0	3.9	2.5	0.0	33	7	0
3990	672	32	58	43	0	0.0	9	5.2	2.8	0.0	0.0	24	5	0
3870	735	26	60	36	0	0.0	9	0.0	2.8	3.3	2.1	28	9	0
3720	767	32	58	46	0	0.0	14	0.0	6.3	2.9	3.0	29	11	0
3620	763	30	70	42	0	0.0	8	7.8	3.1	0.0	0.0	38	0	0
2540	760	32	61	46	0	0.0	6	0.0	3.0	2.3	0.0	30	7	0
3420	751	32	59	37	0	2.4	10	0.0	3.3	2.9	0.0	33	13	0
3240	739	35	55	34	0	0.0	9	0.0	3.3	0.0	0.0	31	13	5
3120	762	66	65	58	11	2.0	14	0.0	5.8	3.0	4.6	29	9	167
3020	769	68	69	58	18	2.4	12	0.0	6.4	2.8	4.3	34	16	74
2930	769	60	67	59	10	4.6	14	6.2	6.6	3.2	5.0	80	37	81
2820	773	66	67	63	11	0.0	12	6.0	6.3	3.6	5.1	31	12	72
2540	779	62	71	57	16	2.2	12	6.1	6.7	2.6	4.4	25	11	103
2440	769	58	74	53	27	2.8	14	5.4	6.2	2.6	5.9	25	16	101
2370	777	61	72	54	20	2.1	12	6.2	6.5	2.6	5.2	26	12	83
2320	785	57	71	51	10	2.6	12	0.0	6.4	2.9	4.1	31	19	78
2160	780	66	76	59	17	3.7	14	5.8	6.8	3.2	4.7	27	15	111
2060	1043	550	222	125	107	19.8	38	9.2	15.6	4.6	9.4	127	66	63
1970	1573	1354	444	262	284	45.8	76	17.3	34.3	8.4	21.9	308	130	70
1890	1325	948	324	199	205	33.3	58	13.2	26.4	6.9	15.6	217	89	145
1730	1161	688	250	157	164	25.3	42	12.9	20.5	6.1	12.2	171	65	209
1560	953	362	172	91	70	17.0	25	7.4	15.0	4.8	13.5	91	38	194
1430	999	440	182	117	104	13.5	27	6.2	13.0	4.4	7.3	102	48	235
1320	788	68	75	69	28	4.0	15	0.0	7.3	3.1	5.6	29	17	416
1210	785	75	76	59	29	4.1	15	0.0	9.3	3.6	0.0	34	12	596
1110	789	100	74	63	40	4.7	15	5.1	9.4	4.4	5.4	28	51	457
930	784	65	73	60	19	4.6	12	0.0	8.0	4.1	6.4	32	16	391
800	782	72	75	69	24	5.0	17	0.0	8.9	4.2	5.7	30	30	476
700	801	82	79	76	34	5.6	17	6.2	10.0	4.0	5.1	36	34	609
570	800	89	80	76	40	6.3	21	7.3	13.0	7.3	0.0	49	18	1313
460	798	91	82	78	39	5.2	21	8.9	12.9	6.9	5.4	28	32	1079
200	809	91	89	92	32	6.7	23	9.2	16.0	10.1	7.3	34	31	1470

ABLE, Arctic Boundary Layer Expedition; pptv, parts per trillion by volume.

those experienced during a regular analysis. Therefore 1275 ml of the whole air working standard was collected on the preconcentration loop in the normal manner, and then a small amount of one or more of the qualitative standards (generally at concentrations in the 1–100 ppmv (10^{-6}) range) were added. The retention times were very reproducible, using this method, usually varying by no more than 0.01 min; except for the augmented peak or peaks, the chromatogram was identical to that of the working standard. In addition, because the plot and DB-1 columns have such different separation characteristics, the elution order of the hydrocarbons is quite dissimilar so that any coelution of gases on one column was most likely resolved on the other. This twofold dissimilar chromatography provided nearly unequivocal peak identification for the C_2-C_6 NMHCs. Response factors for hydrocarbons with the same number of carbons were found to be equivalent. Therefore gases not present in the Scott standards were assigned the same response factors as corresponding carbon number hydrocarbons. As shown in Figures 2, 5, and 6, the FIDs also respond with greatly lessened efficiency to CH_3Cl, N_2O, CCl_2F_2, CCl_3F, and other halocarbons.

Each of the halogenated qualitative standards was in the low ppbv to high pptv range depending on the gas. Although retention times on the DB-624 column were affected less by varying amounts of H_2O and CO_2, qualitative standards were added to the whole air standard in the same manner as were the NMHCs. Only one separation column was used in the halocarbon analysis, but peak symmetry strongly suggests that coelution did not affect the mixing ratios of the seven reported halocarbons.

The specific NMHCs presented in this paper are the

Table 1b. Mixing Ratios for N_2O (ppbv) and Halocarbons (pptv) for Spiral Descent at 51.5°N, 81.8°W, July 17, 1990, ABLE 3B, Mission 4

Altitude, m	N_2O	CFC 12	CFC 11	CFC 113	$CHCl_3$	CH_3CCl_3	CCl_4	C_2Cl_4
5350	316	497	259	75	8.8	140	117	11.1
5200	315	499	262	74	8.8	142	118	11.1
5060	316	491	258	74	8.2	139	116	12.7
4900	315	497	260	74	8.6	139	117	10.8
4770	311	490	260	75	8.6	143	119	11.5
4630	314	487	257	71	8.2	136	114	10.9
4520	312	484	256	73	8.6	137	115	10.7
4380	310	487	257	73	8.6	137	116	10.3
4240	312	488	257	71	8.2	136	115	9.9
4120	313	491	256	74	8.8	133	114	10.5
3990	308	486	257	74	8.2	139	115	10.1
3870	305	476	250	69	9.2	139	111	11.8
3720	304	470	248	69	9.4	137	111	11.9
3620	306	476	249	70	9.2	136	111	11.8
2540	308	480	250	70	9.2	137	111	11.9
3420	311	491	250	74	9.8	142	114	12.3
3240	306	478	252	74	9.8	140	114	12.4
3120	314	489	261	74	10.4	143	116	12.9
3020	N/A	497	261	76	10.8	146	117	13.1
2930	307	487	260	75	10.4	146	119	13.8
2820	315	494	260	74	10.4	145	116	13.0
2540	310	482	259	75	10.0	142	115	12.5
2440	310	491	263	76	10.4	146	118	12.9
2370	310	486	261	74	10.0	142	115	12.5
2320	310	487	262	76	10.8	145	116	12.9
2160	312	494	263	74	10.4	146	118	13.0
2060	313	493	265	77	10.4	146	118	13.1
1970	314	492	264	77	10.8	145	117	12.6
1890	309	486	263	77	10.8	145	116	12.6
1730	312	491	263	77	11.0	147	118	12.8
1560	309	493	259	76	11.0	145	116	12.3
1430	311	491	261	77	10.8	146	117	12.6
1320	311	494	261	77	11.0	146	117	12.8
1210	311	486	262	77	11.4	143	116	12.7
1110	314	483	260	75	11.0	140	114	12.5
930	311	491	262	77	10.8	143	116	12.6
800	308	490	263	79	11.0	145	117	12.9
700	311	488	264	79	11.6	146	117	13.1
570	310	486	264	78	12.0	145	116	12.8
460	312	489	266	79	11.6	146	117	12.9
200	312	492	260	79	12.6	145	116	13.5

Parts per billion by volume (ppbv).

following: ethane (C_2H_6), ethene (C_2H_4), ethyne (C_2H_2), propane (C_3H_8), propene (C_3H_6), propyne (C_3H_4), *n*-butane (*n*-C_4H_{10}), *i*-butane (*i*-C_4H_{10}), 1-butene (1-C_4H_8), *cis*-2-butene (*c*-C_4H_8), *i*-butene (*i*-C_4H_8), *trans*-2-butene (*t*-C_4H_8), 1,3-butadiene (1,3-C_4H_6), *n*-pentane (*n*-C_5H_{12}), *i*-pentane (*i*-C_5H_{12}), 1-pentene (1-C_5H_{10}), isoprene (C_5H_8), *n*-hexane (*n*-C_6H_{14}), 1-hexene (1-C_6H_{12}), benzene (C_6H_6), and toluene (C_7H_8). The assayed halocarbons are dichlorodifluoromethane (CCl_2F_2 or CFC 12), trichlorofluoromethane (CCl_3F or CFC 11), trichlorotrifluoroethane (CCl_2FCClF_2 or CFC 113), chloroform ($CHCl_3$), methylchloroform (CH_3CCl_3), carbon tetrachloride (CCl_4), and perchloroethene (C_2Cl_4). Nitrous oxide was also detected with the ECD.

The precision of the air sample measurements, based on repeated analysis of the NOAA working standard, was estimated to be better than 2% for the C_2-C_5 NMHCs and 10 and 20%, respectively, for benzene and toluene. The halocarbon precision in the NOAA standard was better than ±1% for all reported gases. The standard deviation for CCl_2F_2 in the 37 canister measurements of mission 18 was ±2.9 pptv on a 484 pptv average, or ±0.6% including any atmospheric variability among the samples. The precision in CCl_3F measurements in the same 37 air samples was ±1.7 pptv, or ±0.7%. The precision in the measurement of N_2O was better than ±2%. The three C_2 hydrocarbons were present in all samples collected during this project. Propane and propene suffered from CO_2 peak broadening on the plot column so their detection limits are estimated to be 10 pptv. Because of split ratios and column efficiencies we estimate that the C_4-C_7 hydrocarbons have a lower limit of detection of 2 pptv. The measurements with the plot column (Figures

Table 1c. NMHC Mixing Ratios in Biomass-Burning Plume for Several Hydrocarbons With Concentrations Elsewhere at or Below Detection Limits

Compound[a]	Altitude, m						Weighted Ratio Versus C_2H_6[a]
	2060	1970	1890	1730	1560	1430	
1-C_4H_8	15.2	48.4	34.0	27.1	16.1	12.3	0.05
i-C_4H_8	7.0	21.2	12.4	13.1	9.4	4.2	0.02
1,3-butadiene	8.9	25.2	19.4	17.3	10.2	7.0	0.03
1-pentene[b]	11.2	22.5	18.1	16.4	11.2	9.4	0.02
1-hexene	11	24.3	19.4	16.5	11.0	9.2	0.03

NMHCs, nonmethane hydrocarbons.

[a]The measured yields for *cis*-2-butene, *trans*-2-butene, 2-methylpentane, and 3-methylpentane were below 2 pptv in all air samples. All of these have average yields < 0.01 versus C_2H_6.

[b]The 1-pentene peak had an underlying halocarbon component equivalent to about 5 pptv. The peaks for 1-C_4H_8 and *i*-C_4H_8 have residual values outside the plume canisters which are probably also caused by halocarbons.

2, 4, and 5) of *i*-C_5H_{12}, propyne, *n*-C_5H_{12}, and 1,3-butadiene from several air samples near the detection limits are shown in Figure 7, together with a fire plume enhanced sample. These traces represent air samples from mission 4 (Tables 1*a* and 1*b*) collected at 1970, 2370, 2440, and 3990 m, plus a sample collected at 5440 m just prior to the descent recorded in Tables 1*a* and 1*b*. The mixing ratios for the hydrocarbons in pptv are superimposed in Figure 7. All selected halocarbons were present in all samples at concentrations well above their detection limits.

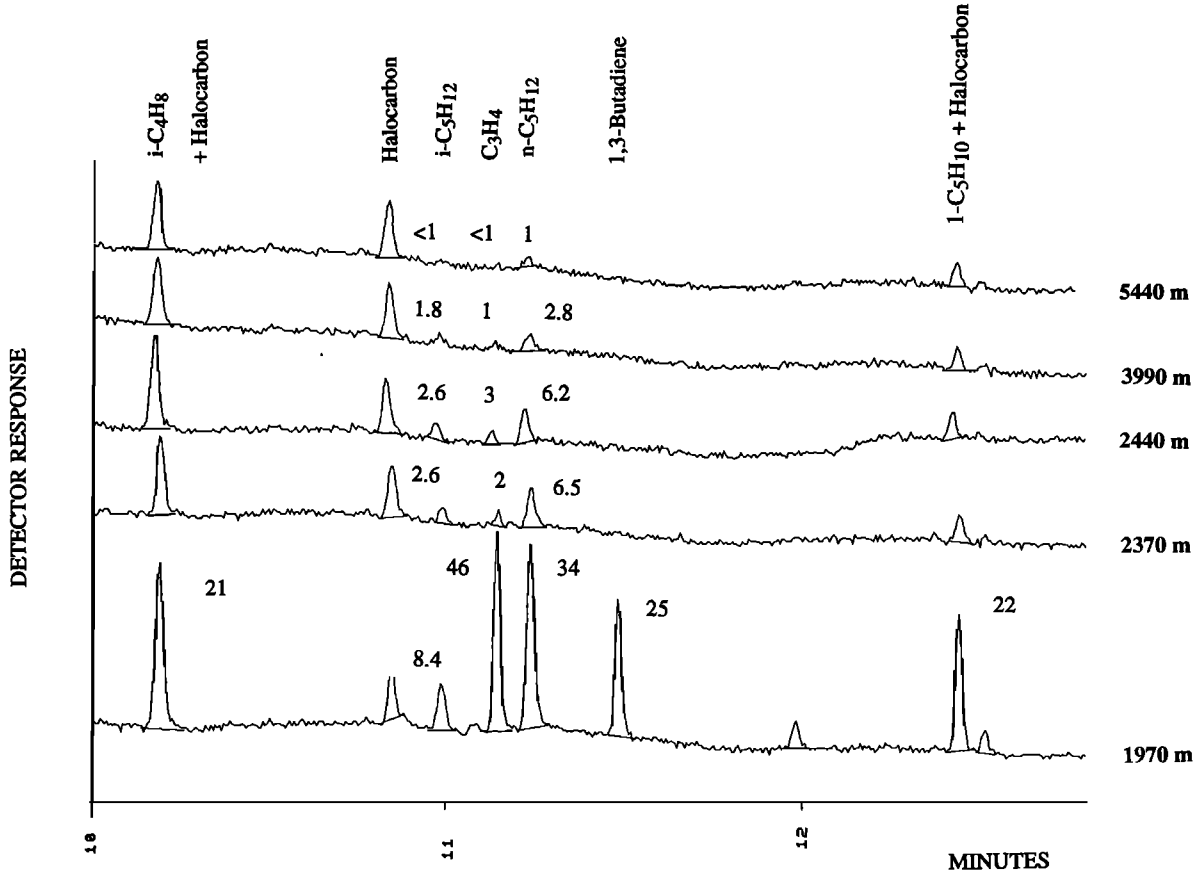

Figure 7. Expanded chromatographic traces of five samples collected inside and outside a biomass-burning plume encountered during mission 4. The numbers next to the traces are the measured mixing ratios for the particular cases. The average altitudes (in meters) at which the samples were collected are given at the end of the chromatograms.

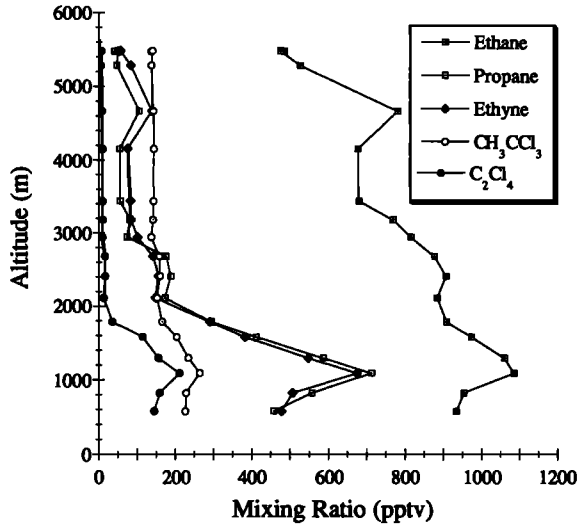

Figure 8. Mixing ratios of ethane, propane, ethyne, CH_3CCl_3, and C_2Cl_4 in parts per trillion by volume (pptv) showing anthropogenic emissions encountered on a vertical descent of mission 21 over 45.5°N latitude and 71.6°W longitude.

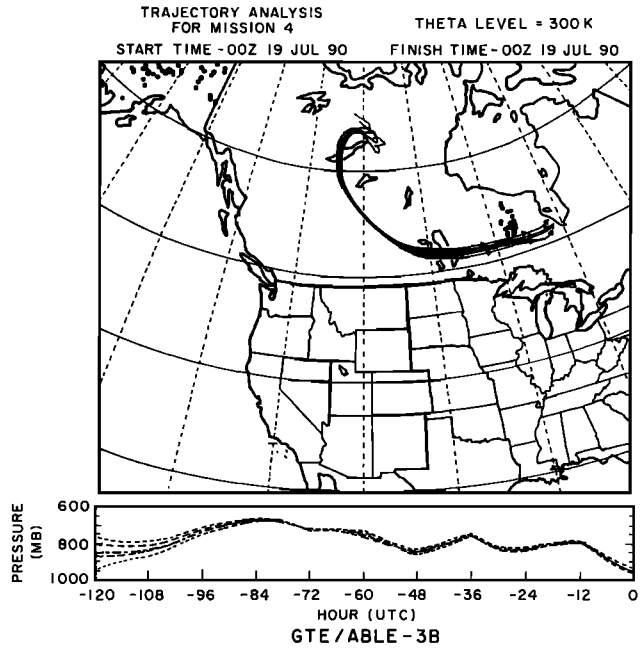

Figure 10. Five-day back trajectories determined by *Shipham et al.* [this issue] showing that the biomass plume encountered on the mission 4 vertical profile originated 12 to 18 hours earlier in western Ontario. The solid circles depict active wild fires burning prior to and during the mission.

Results

Fuel and Burn Description Sites

The type of fuel or vegetation consumed by a fire can play a significant role in determining the partitioning among species of NMHCs emitted. The predominant vegetation type found in the latitudinal belt from 45°N to 70°N is the boreal forest, or taiga. The composition of the boreal forest is mainly pine (*Pinus*), spruce (*Picea*), larch (*Larix*), and fir (*Abies*), mixed, usually after disturbance, with deciduous hardwoods such as birch (*Betula*), poplar (*Populus*), willow (*Salix*), and alder (*Alnus*) and interspersed with extensive lakes and organic terrain [*Stocks*, 1991]. The shaded floor of the boreal forest is covered with moss, lichen, and vascular floras. The terrain surrounding the boreal forest is diverse with a succession from marsh and meadow marsh, through

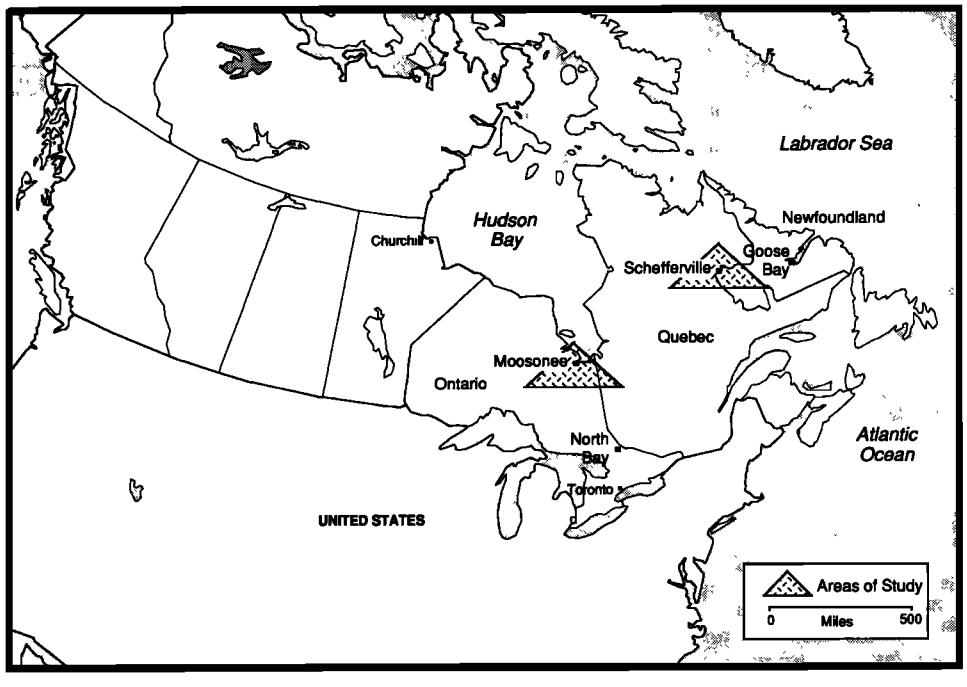

Figure 9. A map displaying the two intensive northern wetland study sites during the Arctic Boundary Layer Expedition 3B campaign: Moosonee, Ontario, and Schefferville, Quebec.

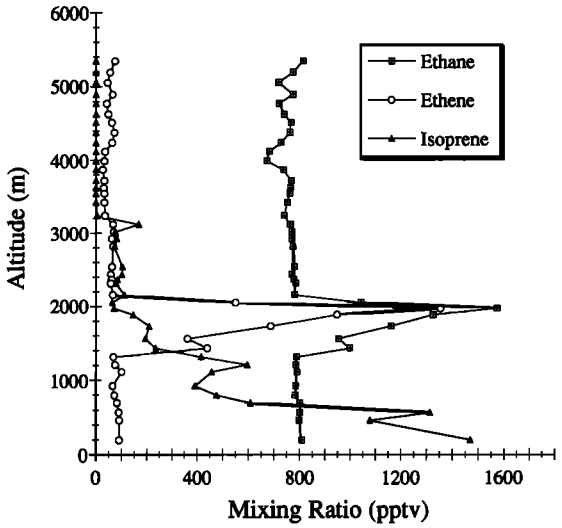

Figure 11. Mixing ratios of ethane, ethene, and isoprene in parts per trillion by volume from a vertical descent on July 17, 1990 (mission 4), over Kinosheo Lake at 51.5°N latitude and 81.8°W longitude.

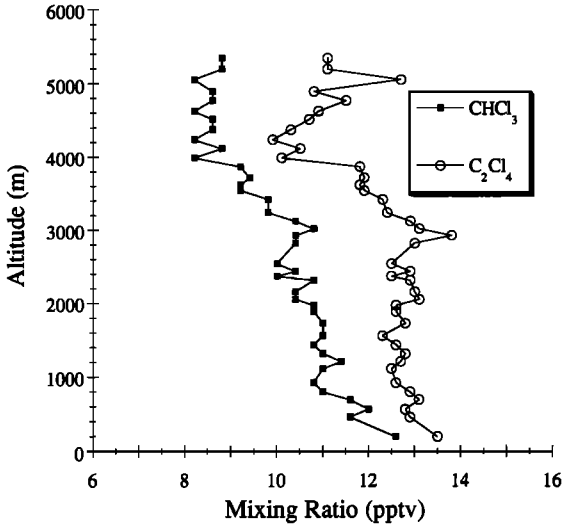

Figure 13. Mixing ratios of $CHCl_3$ and C_2Cl_4 in parts per trillion by volume from a vertical descent on July 17, 1990 (mission 4), over Kinosheo Lake at 51.5°N latitude and 81.8°W longitude.

fen, to bog and swamp, and finally peat. Swamps decrease northward, fens increase northward (and coastward), and tundra and permafrost dominate with increasing latitude [*Riley*, 1982]. To the south, the boreal forest zone is succeeded by temperate forests or grasslands.

Since 1920, detailed forest fire statistics have been archived in Canada. Currently, about 10,000 Canadian fires are reported annually, representing a significant increase over previous decades. This is a reflection not only of a growing population and increased forest use but also of an expanded fire detection capability. Lightning accounts for only 35% of Canada's fires, yet these fires result in 85% of the total area burned. This proportionately larger area of damage occurs because lightning strikes randomly. The location of the fires started in this manner can present access problems usually not associated with human-induced or arson-related fires, delaying their detection and subsequent efforts to extinguish the fire [*Stocks*, 1991].

Case Studies

Consecutive air samples in either horizontal or vertical series often displayed consistent concentrations interrupted by one or several air samples enhanced in NMHCs and sometimes in halocarbons. To distinguish whether measured NMHC enhancements were a result of anthropogenic or biogenic emissions, it is necessary to measure a tracer that is emitted by just one of the sources. Most atmospheric halogenated gases are man-made with uses such that they are given off only in urban areas. However, a distinction needs

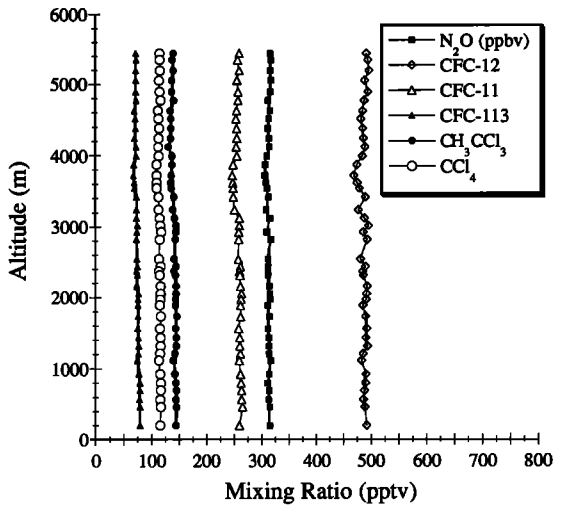

Figure 12. Mixing ratios of N_2O, in parts per billion by volume, CFC 12, CFC 11, CFC 113, $MeCCl_3$, and CCl_4 in parts per trillion by volume from a vertical descent on July 17, 1990 (mission 4), over Kinosheo Lake at 51.5°N latitude and 81.8°W longitude.

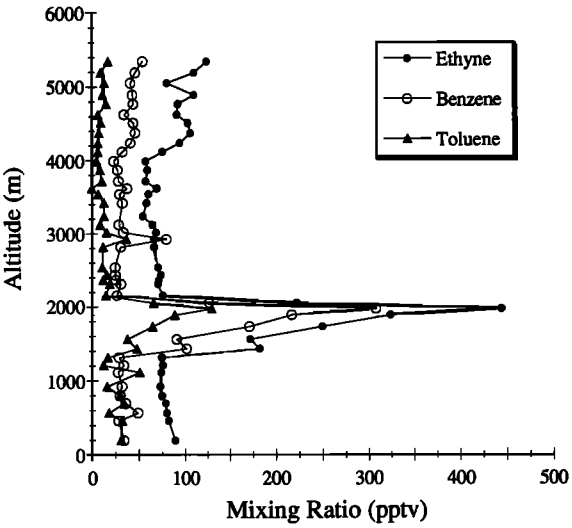

Figure 14. Mixing ratios of ethyne, benzene, toluene in parts per trillion by volume from a vertical descent on July 17, 1990 (mission 4), over Kinosheo Lake at 51.5°N latitude and 81.8°W longitude.

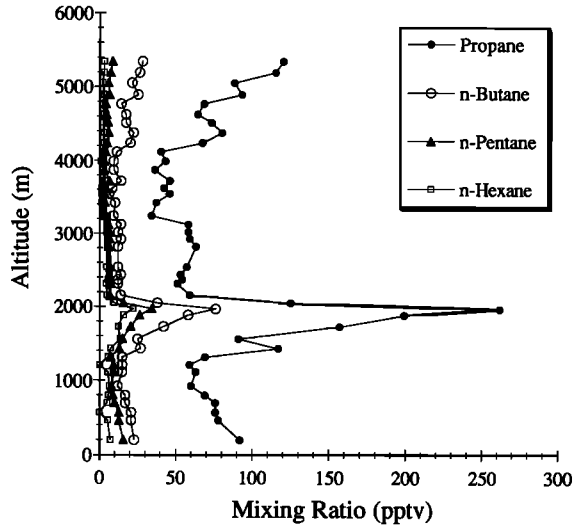

Figure 15. Mixing ratios of propane, *n*-butane, *n*-pentane, and *n*-hexane in parts per trillion by volume from a vertical descent on July 17, 1990 (mission 4), over Kinosheo Lake at 51.5°N latitude and 81.8°W longitude.

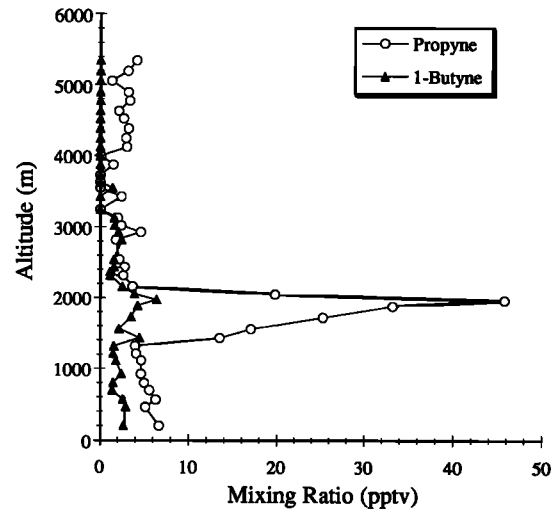

Figure 17. Mixing ratios of propyne and 1-butyne in parts per trillion by volume from a vertical descent on July 17, 1990 (mission 4), over Kinosheo Lake at 51.5°N latitude and 81.8°W longitude.

to be made between fresh plumes coming directly from recent halocarbon augmentation in a nearby urban location and their long-term accumulation from the coalescence of many urban plumes into generalized background levels. Analysis of the samples for various CFCs, CH_3CCl_3, CCl_4, and C_2Cl_4 provides the information necessary to make this distinction. No natural source has been identified for any of these halocarbons, and for most of them the background concentration found throughout the remote atmosphere has steadily increased since their usage began. One example of an air mass recently augmented by urban emissions is shown in Figure 8. The figure reveals enhanced mixing ratios of these halocarbons in the altitude region between 600 and 2000 m, indicating an urban source. Because of its low summertime northern hemisphere background mixing ratio of about 12 ± 2 pptv, ±1% measurement precision and its lifetime of about 6 months, C_2Cl_4 is seen to be a particularly good tracer of anthropogenic emissions. From these analyses, long-range transport of pollutants from urban areas can be established accurately and routinely and is supported by trajectory analysis [*Shipham et al.*, this issue]. When an air mass is encountered exhibiting elevated NMHC concentrations but only background levels of the assayed halocarbons, nonurban combustion is the only reasonable source of the excess concentrations of the NMHCs.

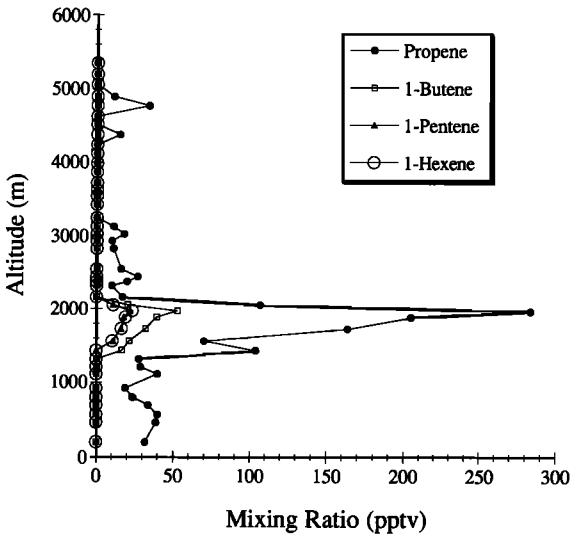

Figure 16. Mixing ratios of propene, 1-butene, 1-pentene, and 1-hexene in parts per trillion by volume from a vertical descent on July 17, 1990 (mission 4), over Kinosheo Lake at 51.5°N latitude and 81.8°W longitude.

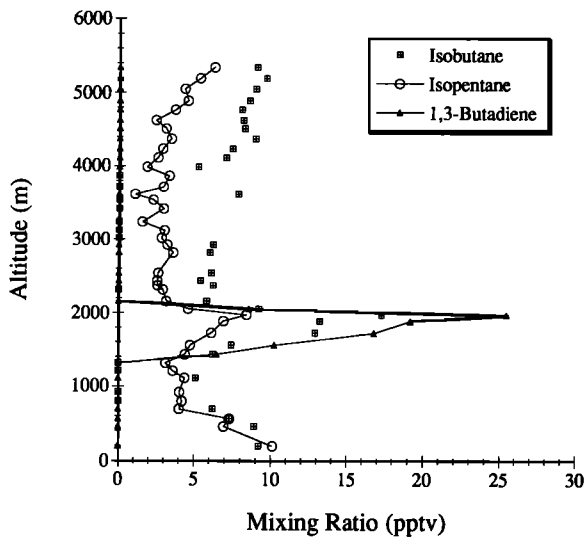

Figure 18. Mixing ratios of isobutane, isopentane, and 1,3-butadiene in parts per trillion by volume from a vertical descent on July 17, 1990 (mission 4), over Kinosheo Lake at 51.5°N latitude and 81.8°W longitude.

Table 2. Emission Factors Relative to Ethane Determined From Six Fire Plume Samples Collected on July 17, 1990 (Mission 4), Over Kinosheo Lake at 51.5°N Latitude and 81.8° Longitude

Hydrocarbon	Average Background Mixing Ratio, pptv	Excess NMHC (pptv) (Δ NMHC) (top) Emission Ratio Relative to C_2H_6 Δ NMHC/ΔC_2H_6 (bottom) Altitude (m) of Sample Collection						Weighted Average Emission Ratio Relative to C_2H_6
		2060	1970	1890	1730	1560	1430	
C_2H_6	782 ± 6	261	791	543	379	171	217	
		1.00	1.00	1.00	1.00	1.00	1.00	(1.00)
C_2H_4	68 ± 13	482	1286	880	620	294	372	
		1.85 ± 0.09	1.63 ± 0.03	1.62 ± 0.04	1.64 ± 0.06	1.72 ± 0.14	1.71 ± 0.11	1.67 ± 0.03
C_2H_2	74 ± 13	148	370	250	176	98	108	
		0.57 ± 0.07	0.47 ± 0.02	0.46 ± 0.04	0.46 ± 0.05	0.57 ± 0.11	0.50 ± 0.09	0.49 ± 0.02
C_3H_8	59 ± 6	66	203	140	98	32	58	
		0.25 ± 0.03	0.26 ± 0.01	0.26 ± 0.02	0.26 ± 0.02	0.19 ± 0.05	0.27 ± 0.04	0.25 ± 0.01
C_3H_6	23 ± 9	84	261	182	141	47	81	
		0.32 ± 0.05	0.33 ± 0.02	0.34 ± 0.03	0.37 ± 0.04	0.27 ± 0.07	0.37 ± 0.06	0.34 ± 0.02
C_3H_4	4 ± 1	16	42	29	21	13	10	
		0.06 ± 0.01	0.05 ± 0.01	0.05 ± 0.01	0.06 ± 0.01	0.08 ± 0.01	0.05 ± 0.01	0.06 ± 0.01
n-C_4H_{10}	14 ± 2	24	62	44	28	11	13	
		0.09 ± 0.01	0.08 ± 0.01	0.08 ± 0.01	0.07 ± 0.01	0.06 ± 0.02	0.06 ± 0.01	0.08 ± 0.01
i-C_4H_{10}	3 ± 1	3	11	10	10	4	3	
		0.01	0.01	0.02	0.03	0.02	0.01	0.02
n-C_5H_{12}	8 ± 1	8	26	18	9	5	7	
		0.03	0.03	0.03	0.02	0.03	0.03	0.03
i-C_5H_{12}	3 ± 1	2	5	4	3	2	1	
		0.01	0.01	0.01	0.01	0.01	0.01	0.01
n-C_6H_{14}	5 ± 1	4	17	11	7	2	4	
		0.02	0.02	0.02	0.02	0.01	0.02	0.02
C_6H_6	29 ± 3	98	279	188	142	62	73	
		0.38 ± 0.02	0.35 ± 0.01	0.35 ± 0.01	0.37 ± 0.01	0.36 ± 0.03	0.34 ± 0.02	0.36 ± 0.01
C_7H_8	20 ± 12	46	110	69	45	18	28	
		0.18 ± 0.07	0.14 ± 0.02	0.13 ± 0.03	0.12 ± 0.05	0.11 ± 0.10	0.13 ± 0.11	0.13 ± 0.02

Biomass-Burning Case Studies

During the ABLE 3B campaign of 1990 a majority of the missions exhibited some influence from local and/or remote forest fires [*Shipham et al.*, this issue]. During this project, approximately one half of the missions focused on the northern Ontario wetlands, while the remaining flights aimed to characterize air masses over Schefferville, Quebec [*Harriss et al.*, this issue] (see Figure 9).

In 1990 the fire season in Ontario, Canada, began around July 15 [*Shipham et al.*, this issue]. The most informative encounter with pristine background air enhanced by a stratified biomass-burning plume occurred during mission 4 on the morning of July 17, 1990, at 51.5°N latitude and 81.9°W longitude, during a vertical descent from 5400 to 150 m above ground level (agl). As the Electra approached Kinosheo Lake (the location of the vertical descent) at 5400 m agl, the lidar detected an optically thick aerosol layer, approximately 900 m thick, between 1300 and 2200 m [*Browell et al.*, this issue]. During the descent this haze layer could be seen to extend in a westward direction to the horizon. Reports were received of forest fires in the area, but none were confirmed visually.

Shipham et al. [this issue] report that during this mission the primary synoptic feature was a strong low-pressure

Table 3. Comparison of Mixing Ratios for Air Samples in the Biomass-Burning Plume From Spiral Descent of Mission 4 Versus Background

Compound, pptv	Background, pptv		Plume	Plume Enhancement
	Above	Below		
CCl_2F_2(CFC 12)	489.7 ± 4.7	488.8 ± 3.4	491.0 ± 2.6	1.8 ± 4.8
CCl_3F(CFC 11)	261.2 ± 1.4	262.4 ± 2.0	262.5 ± 2.2	0.7 ± 2.9
CCl_2FCClF_2(CFC 113)	74.5 ± 0.8	77.8 ± 1.4	76.4 ± 0.6	0.3 ± 2.4
CH_3CCl_3	144.6 ± 1.7	144.3 ± 2.0	145.6 ± 0.8	1.3 ± 2.0
CCl_4	116.7 ± 1.4	116.2 ± 1.0	117.0 ± 0.9	0.6 ± 1.5
C_2Cl_4	13.0 ± 0.4	12.9 ± 0.3	12.7 ± 0.3	−0.2 ± 0.5
N_2O	311.0 ± 2.6 (×10^3)	311.1 ± 1.6 (×10^3)	311.3 ± 2.1 (×10^3)	0.2 ± 2.9

Table 4a. Hydrocarbon Mixing Ratios (pptv) in Biomass-Burning Plumes, ABLE 3B, Missions 9 and 12

Barometric Altitude, m	Ethane	Ethene	Ethyne	Propane	Propene	Propyne	*n*-Butane	*i*-Butane	*n*-Pentane	*n*-Hexane	Benzene	Toluene	Isoprene
Mission 9, July 26, 1990; 51°N, 81.8°W													
710	1083	78	199	214	20	11	50	20	19	<2	78	35	1550
910	1075	72	190	221	21	10	50	19	19	<2	85	30	1831
1030[a]	2229	2898	847	504	890	82	153	35	69	53	534	237	1648
1540	1399	897	426	270	220	33	77	25	30	16	176	70	1260
Mission 12, August 3, 1990; 54.2°N, 65.4°W													
3490	730	26	91	65	<2	2	10	<2	4	<2	44	7	301
3490	980	613	351	98	87	26	25	<2	10	8	135	42	156
3450	827	238	175	83	35	10	13	5	7	<2	85	43	201

[a]Other yields: (mission 9, 1030 m in pptv) 1-C_4H_8, 172; *i*-C_4H_8, 83; *c*-C_4H_8, 28; *t*-C_4H_8, 37; 1,3-butadiene, 150; 1-C_5H_{10}, 72; α-pinene, 435; camphene, 271; β-pinene, 630; sabinene, 77.

system located over northern Saskatchewan/Manitoba, which was responsible for a westerly flow across Ontario. Streamlines at all levels depict a west to northwesterly flow of circumpolar (cP) air being transported around the low, west of Hudson Bay (Figure 10). Satellite imagery depicted clear conditions across Ontario during the early portion of the flight. However, later in the day, cumulus and towering cumulus began to develop and active fires (denoted by the solid circles in Figure 10) burning upstream of the flight path could have accounted for some of the observed haze aloft.

During the mission 4 descent, 41 air samples were collected in 35 min, the results of which are presented in Tables 1*a* and 1*b* and illustrated in Figures 11–18. The data for five hydrocarbons found only in the biomass plume (and for four others not found there either) are summarized in Table 1*c*. Because the background concentrations above and below the plume were very stable, these data serve as an excellent case study for the determination of emission factors for the various species assayed. Figures 11–18 also show a general pattern of constant or slightly increasing concentrations of NMHCs, with the exception of isoprene, with increasing altitude above the Canadian wetlands. These results are similar to those obtained in ABLE 3A, STRATOS II and III, and other studies at generally higher northern latitudes [*Rasmussen et al.*, 1983; *Ehhalt et al.*, 1985; *Rudolph*, 1988; *Blake et al.*, 1992] which showed a positive correlation of mixing ratio with altitude. The presence of the short-lived molecule, isoprene, observed throughout the planetary boundary layer (PBL) on mission 4 (see Figure 11) suggests that vertical mixing within and up to the PBL was rapid. Isoprene, which is emitted by vegetation within the boreal forest, is not observed above the PBL and distant from the forests, illustrating its use as a local tracer. The biomass plume encountered during the vertical descent of mission 4 occurred between 1300 and 2200 m altitude (see Figures 11–18). Based on the back trajectories [*Shipham et al.*, this issue], the plume encountered at the location of the vertical descent was approximately 12 to 18 hours old (see Figure 10). The back trajectories suggest that the air mass passed directly over fires prior to arriving at the sampling location. Thus the plume encountered between 1300 and 2200 m probably went aloft around sunset the previous day. Therefore as the main removal process for most NMHCs is reaction with hydroxyl radicals only produced during the daytime, it is likely that such removal occurred for just a few hours prior to sample collection. Thus only the shortest-lived gases had undergone significant removal. The absence of *cis*-2-butene and *trans*-2-butene, both highly reactive with hydroxyl, support this conclusion.

The mixing ratios given in Tables 1*a* and 1*b* provide an excellent set of data for determination of relative biomass-burning emission factors for the less reactive hydrocarbons, while providing little information about the absolute amounts involved per unit weight of forest burned. Between 3200 and 200 m the mixing ratios of C_2H_6 exhibit only small variations and are nearly constant, 783 ± 13 pptv, except between the plume altitudes of 1300–2200 m. If the next five canisters each above and below the plume are averaged, the C_2H_6 values are even more tightly bunched at 782 ± 6 pptv. Similar observations of relatively small variations, except in the plume canisters, are recorded for all other hydrocarbons (except isoprene) in Table 2. With its atmospheric lifetime of a few hours or less, the isoprene concentrations in the

Table 4b. Halocarbon and N_2O Mixing Ratios (ppbv), ABLE 3B Missions 9 and 12

Barometric Altitude, m	N_2O	CFC 12	CFC 11	CFC 113	$CHCl_3$	CH_3CCl_3	CCl_4	C_2Cl_4
Mission 9, July 26, 1990; 51°N, 81.8°W								
710	302	485	263	73	12.6	145	117	11.9
910	312	488	265	72	12.8	146	117	12.1
1030	308	489	264	76	13.2	146	118	12.6
1540	310	489	265	77	12.6	141	114	12.3
Mission 12, August 3, 1990; 54.2°N, 65.4°W								
3490	310	490	265	72	10.0	141	116	11.4
3490	309	495	265	73	9.8	141	116	11.8
3500	313	488	266	73	10.8	146	118	11.7

mission 4 spiral were certainly the consequence of very recent injections, presumably mixed upward prior to the arrival of the biomass-burning plume. While isoprene, or 2-methyl-1,3-butadiene, is a plausible compound to have been emitted from a burning forest, as its close chemical relative 1,3-butadiene definitely is, the isoprene levels within the plume samples show no evidence of any special enhancement. In fact, the major plume canister at 1970 m had a lower isoprene concentration than most of the other plume canisters.

Excess NMHC mixing ratios have been calculated in Table 2, for the six plume canisters, using the assumption that the background concentrations in the absence of biomass burning would have been the average value for the 10 canisters surrounding them, five above and five below. These excess NMHC values have then been converted, also in Table 2, into relative excesses versus ΔC_2H_6. (Emission factors are normally reported relative to CO or CO_2. However, CO_2 was not an on-board measurement and the carbon monoxide instrument was in a calibration mode during some of the plume events. Because of this we have chosen to report our NMHC emission factors relative to ethane.) The errors of these relative excesses have been estimated by the arbitrary assumption that the standard deviation for the individual canister in the plume is the same as for the background canisters, e.g., at 2060 m $[C_2H_6] = (1043 \pm 6) -$

Table 5. NMHC Emission Ratio Relative to C_2H_6 in Biomass-Burning Plumes

	Mission 4 Spiral	Mission 9 Spiral	Mission 12 3490 m	Mission 9 Moosonee Spiral "Aged"	Mission 11 Spiral "Aged"
Number of samples	6	2	2	3	3
Ethane	1.00	1.00	1.00	1.00	1.00
Ethene	1.67	2.45	2.30	0.00	0.20
Ethyne	0.49	0.57	0.99	0.39	0.48
Propane	0.25	0.25	0.15	0.43	0.40
Propene	0.34	0.73	0.32	0.00	0.02
Propyne	0.06	0.06	0.09	0.01	0.02
n-Butane[a]	0.08	0.09	0.05	0.10	0.13
i-Butane	0.02	0.01	<0.01	0.04	0.06
1-Butene	0.06	0.14	0.04	0.00	<0.01
c-2-Butene	<0.01	0.02	<0.01	0.00	<0.01
t-2-Butene	<0.01	0.03	<0.01	0.00	<0.01
i-Butene	0.00	0.07	0.02	0.00	0.00
1,3-Butadiene	0.03	0.12	0.00	0.00	0.00
n-Pentane	0.03	0.05	0.02	0.02	0.04
i-Pentane	0.01	0.03	0.00	0.03	0.02
1-Pentene	0.02	0.06	0.01	0.00	0.01
n-Hexane	0.03	0.05	0.02	<0.01	0.01
2-MethylPentane	<0.01	<0.01	<0.01	0.00	<0.01
3-MethylPentane	0.00	0.00	0.00	0.00	0.00
1-Hexene	0.03	0.07	0.02	0.00	0.01
Benzene	0.36	0.37	0.38	0.17	0.21
Toluene	0.13	0.16	0.20	0.00	0.02
Maximum enhancement of C_2H_6, pptv	791	1150	250	350	1500
Average plume C_2Cl_4, pptv	12.6	13.0	12.0	12.5	12.0

[a]When a trace peak is present but too small to integrate, the entry reads <0.01; when there is no indication of a peak at all, the entry reads 0.00.

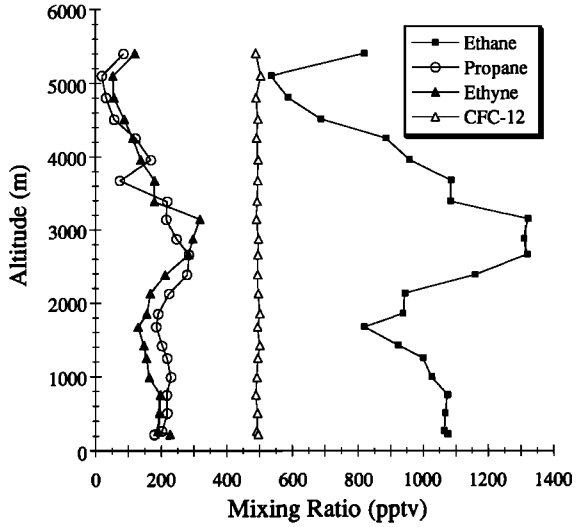

Figure 19. Mixing ratios of ethane, propane, ethyne, and CFC 12 in parts per trillion by volume from a vertical descent on July 26, 1990 (mission 9), over Kinosheo Lake at 51.6°N latitude and 81.6°W longitude.

(782 ± 6) = (261 ± 8.5) and $[C_2H_4]$ = (550 ± 13) − (68 ± 13) = (482 ± 18), for a ratio of 1.85 ± 0.09. The weighted average in the final column has been calculated by summing all of the excess NMHC values in all six plume canisters and taking the ratios of these sums.

Alternatively, least squares fits to the C_2H_6 and C_2H_4 mixing ratios below 3200 m, excluding the plume canisters, have formulas of (803.1–1.15x) and (88.8–0.97x), with x equal to the altitude in hundreds of meters. The standard deviations for these fits are smaller, ±4.4 and ±8.4 pptv, respectively, than for the assumed constant values of Table 2, but the calculated $[C_2H_4]/[C_2H_6]$ ratios are affected marginally by the change in background assumption, with the largest variation a value of 1.82 instead of 1.85 for 2060 m. The weighted average ratio is 1.66 with this least squares background assumption, whereas it is 1.67 without it.

The relative amounts of excess hydrocarbon in these six canisters are very consistent as shown by the near constancy of all of the ratios in Table 2. This consistency holds quite well, not only for the components such as C_2H_6, C_2H_4 and C_2H_2 but also for several of the less abundant hydrocarbons, even for those with single-digit pptv excesses. The calculated errors for toluene are clearly too large and are reduced to the ±0.02 level if a background of 15 ± 3 is used, ignoring the sample at 1110 m.

In contrast to the observations for NMHC the plume canisters from the mission 4 spiral show no statistically significant excesses of N_2O or of the man-made chlorocarbons, as summarized in Table 3. The average mixing ratios of these have been calculated for nine canisters each above and below the plume canisters, and the average of all 18 has been subtracted as the background for the plume samples. None of these calculated "excesses" approaches even the 1σ level of significance. Furthermore, 33% of the total C_2H_6 excess occurs in one canister (1970 m) and 73% in three (1970, 1890, 1730 m) of the six canisters, and no differences exist in concentrations observed for these three versus the other three plume canisters. No evidence, therefore, exists for the release of N_2O or the reported halocarbons during forest fires in northern Ontario. This conclusion differs from that of *Hegg et al.* [1990], whose data were largely drawn from fires in the vicinity of Los Angeles. As a minimum, the lack of any enhanced halocarbon emission indicates that extrapolation from the Los Angeles vicinity as globally typical is inappropriate. Further data from other locations are highly desirable, including a recheck of Los Angeles fires.

Missions which took place later in the fire season revealed elevated background levels of CO, NO_x, NO_y, and several of the longer-lived NMHCs. The enhanced background levels of these gases precluded the same treatment as that used for mission 4 samples because the emission ratio determinations are all based on differences with respect to background. This problem is minimized when the measured in-plume mixing ratios are large.

Biomass plumes were encountered during many of the missions but often were mixed with urban air, as inferred from elevated concentrations of C_2Cl_4, thus distorting the NMHC ratios. For this study, only plumes which were visually verified to be of biomass-burning origin or plumes for which the trajectory analyses are unequivocal have been used for emission factor calculations. In both cases the assignment to biomass burning has been confirmed by the lack of change in halocarbon concentrations, especially C_2Cl_4, from background levels. In addition to the mission 4 spiral, samples obtained from missions 9 and 12 meet these three stringent criteria for biomass plumes. The low-altitude samples of mission 9 were taken in a plume rising directly from a visible active fire and were, thus, only a few minutes old. The observed yield of 1,3-butadiene in the most impacted canister of mission 9 had a concentration ratio of 0.13 versus C_2H_6. The emission yields from this canister are, because of the proximity in both time and space of the sampling to the fire, probably the best estimate we have of the initial yields in an active Canadian forest fire. In none of these other occurrences were as many separate samples

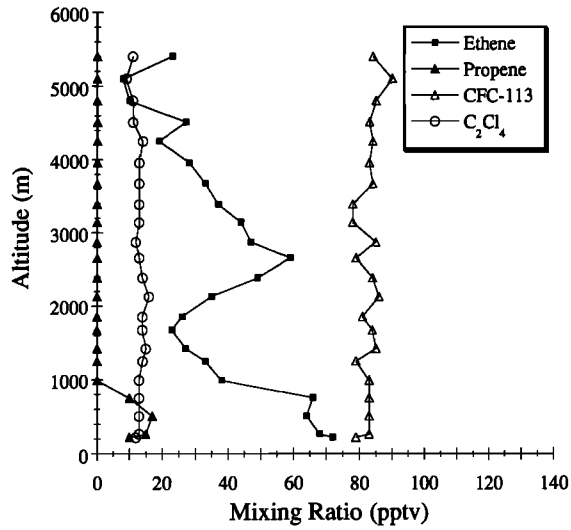

Figure 20. Mixing ratios of ethene, propene, CFC 113, and C_2Cl_4 in parts per trillion by volume from a vertical descent on July 26, 1990 (mission 9), over Kinosheo Lake at 51.6°N latitude and 81.6°W longitude.

Table 6. Relative NMHC Enhancements (versus C_2H_6) in Biomass-Burning Plumes, Literature

	Bonsang Aircraft January 13, 1989, Africa, 200 m	Bonsang Ground January 1989 Africa	*Radke et al.* [1991] Aircraft Hardiman Fire	*Radke et al.* [1991] Aircraft Battersby Fire	*Radke et al.* [1991] Aircraft Wickstead Fire	*Blake et al.* [1992] Boreal Forests ABLE 3A Alaska
Ethane	1.00	1.00	1.00	1.00	1.00	1.00
Ethene	2.03	4.77				
Ethyne	0.60	1.80	0.80	0.67	0.50	0.38
Propane	0.31	0.16	0.27	0.32	0.23	0.08
Propene	0.55	0.77	0.92	1.13	0.87	<0.01
n-Butane	0.14	0.04	0.02	0.06	0.04	
i-Butane	0.04	0.01				
1-Butene	0.15	0.12				
t-2-Butene	0.04	0.03				
c-2-Butene	0.03	0.02				
1,3-Butadiene	0.04	0.18				
n-Pentane	0.07	0.03				
i-Pentane	0.12	0.10				
1-Pentene	0.08	0.03				
2-MePentane	0.02	0.01				
3-MePentane	0.01	<0.01				
n-Hexane	0.02	0.05				
1-Hexene	0.05	0.02				
Methane		59.1	7.9	18.4	14.0	33.0
Carbon monoxide		321	196	330	116	

Table 7. Hydroxyl Removal by Reactions with NMHC Compounds

		HO Removal Rate, s^{-1}		
Compound	HO Rate Constant	1970 m Mission 4	200 m Mission 4	1030 m Mission 9
C_2H_6	2.2 (−13)	0.007	0.004	0.012
C_2H_4	8.8 (−12)	0.25	0.020	0.61
C_2H_2	7.8 (−13)	0.007	0.002	0.016
C_3H_8	1.2 (−12)	0.006	0.003	0.014
C_3H_6	2.9 (−11)	0.17	0.022	0.62
C_3H_4	5.6 (−12)	0.005	0.001	0.011
n-C_4H_{10}	2.3 (−12)	0.004	0.001	0.009
i-C_4H_{10}	2.2 (−12)	0.001	0.001	0.002
1-C_4H_8	3.5 (−11)	0.038	<0.003	0.14
i-C_4H_8	4.0 (−11)	...	...	0.08
c-C_4H_8	6.0 (−11)	...	...	0.04
t-C_4H_8	7.0 (−11)	...	...	0.06
1,3-Butadiene	7.3 (−11)	0.038	...	0.26
n-C_5H_{12}	3.7 (−12)	0.003	0.001	0.006
i-C_5H_{12}	3.7 (−12)	0.001	0.001	0.001
1-C_5H_{10}	3.0 (−11)	0.014	<0.003	0.05
Isoprene	1.1 (−10)	0.16	4.0	4.3
n-C_6H_{14}	5.2 (−12)	0.002	0.001	0.007
1-Hexene	3.5 (−11)	0.017	<0.003	0.07
Benzene	1.2 (−12)	0.008	0.001	0.015
Toluene	6.4 (−12)	0.017	0.005	0.036
Terpenes	1.0 (−10)	>0.2	>3.6	>3.3
CH_4[a]	8.0 (−15)	0.3	0.3	0.3
CO[a]	2.4 (−13)	1.4	0.6	>1.0

All rate constant values were for 298 K and obtained from *Atkinson* [1990] and *DeMore* [1992].

[a] *Harriss et al.* [this issue].

Table 8. Estimated Annual Emissions for Selected C_2-C_4 Hydrocarbons Resulting From Biomass Buring

Compound	$\Delta i/\Delta CO$[a]	Circumpolar[b] Emissions From Biomass Burning, 10^{10} g	Global[c] Biomass Emissions, 10^{12} g
C_2H_6	4.0×10^{-3}	2.3	1.5
C_2H_2	2.3×10^{-3}	1.1	0.7
C_3H_8	1.0×10^{-3}	0.8	0.6
n-C_4H_{10}	3.0×10^{-4}	0.3	0.2

[a]Carbon monoxide values from *Harriss et al.* [this issue].
[b]Assumes 1.8×10^{11} moles of CO released in circumpolar regions during biomass burning [*Stocks*, 1991; *Andreae*, 1991].
[c]Assumes 1.5% of global biomass-burning emissions occur in circumpolar regions.

collected as in the plume shown in Tables 1*a* and 1*b*, thus the consistency checks of Table 2 are not possible. The data on individual compounds are summarized in Tables 4*a* and 4*b* for four canisters on a short ascent on mission 9 and for three successive canisters in level flight on mission 12. Two of the canisters contained plume samples in each set, while the others serve as background. These data have been calculated in the manner used in Table 2. The emission ratios relative to C_2H_6 are summarized for all three missions in Table 5.

On a number of missions, plumes were encountered that through trajectory analysis were later attributed to biomass burning. However, these plumes were "aged", having last come in contact with a fire at least five days before the mission was flown. These older plumes have a very different NMHC signature, as seen in Figures 19 and 20. The more reactive gases show little or no enhancement, while the longer-lived gases are observed in appreciable amounts. Clearly, emission factors for the most reactive gases such as 1,3-butadiene are usually no more than lower limit unless the plume is sampled in a time short compared to the individual atmospheric lifetime. However, emission factors for the longer-lived gases, ethyne and propane, are generally in good agreement with those measured in fresh plume samples. Emission factors for samples collected in aged plumes, mission 9 near Moosonee and mission 11 over Schefferville, are given in Table 5 for comparison.

The NMHC composition of recently augmented air from fires characterized during ABLE 3B (Table 5), exhibited a relatively low variability, which denotes the existence of a typical signature. On a volume-to-volume basis of all the NMHCs assayed, ethene was the dominant hydrocarbon emitted (33.5 ± 4.9%); C_2H_6 is produced also in substantial amounts (20.2 ± 1.9%); then C_2H_2 (7.6 ± 4.9%), C_3H_6 (8.2 ± 2.1%), C_6H_6 (7.2 ± 1.2%), C_3H_8 (5.4 ± 1.9%), and C_7H_8 (3.1 ± 1.1%), making up the majority of the volatile species released during biomass burning. These data are in good agreement with other published results [*Crutzen et al.*, 1985; *Bonsang et al.*, 1991].

Various types of fires from different regions have been studied by numerous groups [*Bonsang et al.*, 1991; *Radke et al.*, 1991; *Blake et al.*, 1992]. Emission factors from some of these studies are given in Table 6. Although the emission factors from these other studies exhibit considerable scatter, a significant amount of which probably originates from differently aged plumes, the values agree fairly well.

The impact of biomass-burning plumes on local photochemistry is illustrated in Table 7. The relative removal rate by HO radical reaction has been calculated for each of the NMHC compounds measured by us for several typical biomass-burning samples. When isoprene is present, its reactions tend to dominate the NMHC hydroxyl budget, although in a few instances the incremental additions from biomass burning play a comparable role in total reactivity. The reactions of HO radicals with CH_4 and CO are major contributors in all cases. However, NMHCs released by biomass burning can play a significant role in regional photochemistry long after isoprene and the reactive alkenes, etc., have been removed.

World Average Calculation

Biomass-burning emission factors for CO and NMHCs are dependent on many factors, particularly the fuel and whether the fire is flaming or smoldering. Because the efficiency of a flaming fire is greater than a smoldering one, the CO_2/CO emission ratio is greater in the former case [*Einfeld et al.*, 1991]. In this study we assume that the encountered plumes were a result of both flaming and smoldering fires and that the emission factors obtained in this study represent the average.

Savanna fires would burn hot and fast and are therefore very efficient and produce relatively high amounts of CO_2 [*Einfeld et al.*, 1991]. Thus although savanna fires represent a significant amount of total biomass burned, it is likely that biomass burning of forested areas produce the majority of CO emitted during fires. If it is assumed that NMHC and CO emissions from biomass burning in different regions of the world are similar and that 350×10^{12} g of CO are released globally each year during biomass burning [*Andreae*, 1991], then the contribution of biomass-burning emissions to the tropospheric budgets of some of the longer-lived gases can be estimated. The $\Delta CO/\Delta C_2H_6$ biomass-burning ratio obtained in this project is 260, while the average of the four geographically different studies given in Table 6 is 240 ± 120 [*Stocks*, 1991; *Harriss et al.*, this issue]. Thus if the ratio $\Delta CO/\Delta C_2H_6$ is taken to be fixed for all biomass fires at an average value of 250 ± 90, then the global biomass-burning source strength of C_2H_6 can be estimated in the following way:

$$\left(\frac{1}{250}\right) 350 \times 10^{12} \text{ g/y} \left(\frac{30 \text{ g/mole}}{28 \text{ g/mole}}\right) = 1.5 \times 10^{12} \text{ gC}_2\text{H}_6\text{/y}$$

This number can then be compared to the $13 \pm 3 \times 10^{12}$ g annual global release of C_2H_6 estimated by *Blake and Rowland* [1986], from which a percent contribution to annual C_2H_6 emissions from biomass burning of 9–15% is calculated. Using emission ratios obtained in this study, the global input of C_2H_2, C_3H_8, and n-C_4H_{10} were calculated in the same manner as was C_2H_6 and are given in Table 8. Using latitudinal profiles of our unpublished data and those from *Singh and Zimmerman* [1992], global input values for ethyne, propane, and n-butane of 7–10%, 3–4%, and 1–2%, respectively, are obtained.

Conclusions

In conclusion, the following observations were made during the ABLE 3B campaign which took place during July and August 1990 over the northern Canadian wetlands. Based on many vertical characterizations of the background conditions encountered during this experiment, the general trend was for the concentrations of halocarbons and NMHCs to be nearly constant or slightly increasing with increasing altitude (up to 5400 m). The vertical profile of isoprene implies that mixing within the boundary layer was rapid to altitudes as high as 3000 m. Stratified layers denoting long-range transport were evident. Based on the levels of C_2Cl_4 and related anthropogenic halocarbons, the origin of these stratified layers or plumes may be further characterized as having either biogenic and/or urban/industrial sources. Emission factors for NMHCs were calculated and ethene was found to be the most abundant species released. During biomass burning, alkanes, alkenes, and alkynes are all emitted in significant quantities. The correlation coefficients for the longer-lived gases are in excellent agreement and for the shorter-lived species are very good. Compounds such as CFC 12, N_2O, and isoprene, whose emissions from biomass burning have been reported in previous studies, were not found to be enhanced significantly in the fire plumes encountered. The estimated percent contribution of biomass-burning emissions to the worldwide total were calculated for ethane, ethyne, propane, and *n*-butane to be 9–15%, 7–10%, 3–4%, and 1–2%, respectively. Finally, the less reactive NMHCs associated with biomass burning tend to accumulate as the fire season progresses. Although these emissions can effect regional photochemistry, within the PBL, isoprene is still the dominant hydroxyl sink.

Acknowledgments. The authors greatly appreciate C. DeSantis, M. Lucero, and M. McEachern who participated in the analytical processing throughout the mission at Canadore College, North Bay, Ontario, Canada. We thank the following research group members for their assistance in the fabrication of the experimental apparatus, comments regarding the manuscript, and support during the field mission: T. Merrill, P. Russell, M. Zondlo, B. McGoveney, and B. Chisholm, N. Blake, R. Iyer, J. Wang, and N. Wang. We are indebted to Ralph Kolbush, Director of the UCI Machine Shop, for excellent support before, during, and after the missions. We thank J & W Scientific for the use of the experimental 75 DB-624 column. The opportunistic filling of air canisters when an interesting atmospheric air parcel was encountered by the Electra was dependent upon the timely relay of information from the operators of real-time, on-board instrumentation. We especially thank Mark Poudrier, Peter Brown, and the rest of the personnel at Canadore College for the use of their laboratory space and for their frequent assistance with items in logistical support of the analytical laboratory. This work was supported by funds from the National Aeronautics and Space Administration (NASA) grant NAG-1-783.

References

Aikin, A. C., J. B. Herman, E. J. Maier, and C. J. McQuillan, Atmospheric chemistry of ethane and ethylene, *J. Geophys. Res.*, *87*, 3105–3118, 1982.

Andreae, M. O., Biomass burning: Its history, use, and distribution and its impact on environmental quality and global climate, in *Global Biomass Burning: Atmospheric, Climatic and Biospheric Implications*, edited by J. S. Levine, pp. 3–21, MIT Press, 1991.

Andreae, M. O., et al., Biomass-burning emissions and associated haze layers over Amazonia, *J. Geophys. Res.*, *93*, 1509–1527, 1988.

Atkinson, R., Kinetics and mechanisms of the gas-phase reactions of the hydroxyl radical with organic compounds under atmospheric conditions, *Chem. Rev.*, *85*, 69–201, 1986.

Barrie, L. A., Arctic air pollution: An overview of current knowledge, *Atmos. Environ.*, *20*, 643–663, 1986.

Barrie, L. A., and R. M. Hoff, Five years of air chemistry observations in the Canadian Arctic, *Atmos. Environ.*, *19*, 1995–2010, 1985.

Blake, D. R., and F. S. Rowland, Global atmospheric concentrations and source strength of ethane, *Nature*, *321*, 231–233, 1986.

Blake, D. R., D. Hurst, T. W. Smith, Jr., W. J. Whipple, T. Y. Chen, N. J. Blake, and F. S. Rowland, Summertime measurements of selected nonmethane hydrocarbons in the Arctic and subarctic during the 1988 Arctic Boundary Layer Expedition (ABLE 3A), *J. Geophys. Res.*, *97*, 16,559–16,588, 1992.

Bonsang, B., G. Lambert, and C. C. Boissard, Light hydrocarbon emissions from African savannah burnings, in *Global Biomass Burning: Atmospheric, Climatic and Biospheric Implications*, edited by J. S. Levine, pp. 155–161, MIT Press, Cambridge, Mass., 1991.

Browell, E. V., M. A. Fenn, C. F. Butler, W. B. Grant, R. C. Harriss, and M. C. Shipham, Ozone and aerosol distributions in the summertime troposphere over Canada, *J. Geophys. Res.*, this issue.

Cofer, W. R. III, J. S. Levine, P. J. Riggan, D. I. Sebacher, E. L. Winstead, E. F. Shaw, J. A. Brass, and V. G. Ambrosia, Trace gas emissions from a midlatitude chaparral fire, *J. Geophys. Res.*, *93*, 1653–1658, 1988.

Cofer, W. R. III, J. S. Levine, D. I. Sebacher, E. L. Winstead, P. J. Riggan, B. J. Stocks, J. A. Brass, V. G. Ambrosia, and P. J. Boston, Trace gas emissions from chaparral fire and boreal forest fires, *J. Geophys. Res.*, *94*, 2255–2259, 1989.

Crutzen, P. J., and M. O. Andreae, Biomass burning in the tropics: Impact on atmospheric chemistry and biogeochemical cycles, *Science*, *94*, 1669–1678, 1990.

Crutzen, P. J., and J. Fishman, Average concentrations of OH in the troposphere and the budgets of CH_4, CO, H_2 and CH_3CCl_3, *Geophys. Res. Lett.*, *4*, 321–324, 1977.

Crutzen, P. J., L. E. Heidt, J. P. Krasnec, W. H. Pollock, and W. Seiler, Biomass burning as a source of atmospheric gases CO, H_2, N_2O, CH_3Cl and COS, *Nature*, *282*, 253–256, 1979.

Crutzen, P. J., A. C. Delany, J. Greenberg, P. Haagenson, L. Heidt, R. Lueb, W. Pollock, W. Seiler, A. Wartburg, and P. Zimmerman, Tropospheric chemical composition measurements in Brazil during the dry season, *J. Atmos. Chem.*, *2*, 233–256, 1985.

Delany, A. C., P. Haagensen, S. Walters, A. F. Wartburg, and P. J. Crutzen, Photochemically produced ozone in the emission from large-scale tropical vegetation fires, *J. Geophys. Res.*, *90*, 2425–2429, 1985.

Delmas, R., On the emission of carbon, nitrogen, and sulfur in the atmosphere during bushfires in intertropical savannah zones, *Geophys. Res. Lett.*, *9*, 761–764, 1982.

DeMore, W. B., S. P. Sander, D. M. Golden, R. F. Hampson, M. J. Kurylo, C. J. Howard, A. R. Ravishankara, C. E. Kolb, and M. J. Molina, Chemical kinetics and photochemical data for use in stratospheric modeling, in Evaluation 10, *JPL-92-20*, NASA Jet Propul. Lab., Washington, D. C., August 15, 1992.

Ehhalt, D. H., J. Rudolph, F. X. Meixner, and U. Schmidt, Measurements of selected C_2-C_5 hydrocarbons in the background troposphere: Vertical and latitudinal variations, *J. Atmos. Chem.*, *3*, 29–52, 1985.

Einfeld, W., D. E. Ward, and C. Hardy, Effects of fire behavior on prescribed fire smoke characteristics: A case study, in *Global Biomass Burning: Atmospheric, Climatic and Biospheric Implications*, edited by J. S. Levine, pp. 412–419, MIT Press, 1991.

Farman, J. C., B. G. Gardiner, and J. D. Shanklin, Large losses of total ozone in Antarctica reveal seasonal ClO_x/NO_x interaction, *Nature*, *315*, 207–210, 1985.

Galloway, J. N., and G. E. Likens, Acid precipitation: The importance of nitric acid, *Atmos. Environ.*, *15*, 1081–1085, 1981.

Gilpin, T. J., Global tropospheric concentrations of three chlorofluorocarbons: 1984–1988, Ph.D. dissertation, Univ. of Calif., Irvine, 1991.

Greenberg, J. P., and P. R. Zimmerman, Nonmethane hydrocarbons in remote tropical, continental and marine atmospheres, *J. Geophys. Res.*, *89*, 4767–4778, 1984.

Greenberg, J. P., P. R. Zimmerman, L. Heidt, and W. Pollock,

Hydrocarbon and carbon monoxide emissions from biomass burning in Brazil, *J. Geophys. Res.*, *89*, 1350–1354, 1984.

Greenberg, J. P., P. R. Zimmerman, and R. B. Chatfield, Hydrocarbons and carbon monoxide in African savannah air, *Geophys. Res. Lett.*, *12*, 113–116, 1985.

Greenberg, J. P., P. R. Zimmerman, and P. Haagenson, Tropospheric hydrocarbon and CO profiles over the U.S. West Coast and Alaska, *J. Geophys. Res.*, *95*, 14,015–14,026, 1990.

Greenberg, J. P., P. R. Zimmerman, W. Pollock, R. A. Lueb, and L. Heidt, Diurnal variability of atmospheric methane, nonmethane hydrocarbons, and carbon monoxide at Mauna Loa, *J. Geophys. Res.*, *97*, 10,395–10,413, 1992.

Hansen, J., A. Lacis, and M. Aathe, Greenhouse effect of chlorofluorocarbons and other trace gases, *J. Geophys. Res.*, *94*, 16,417–16,421, 1989.

Harriss, R. C., S. C. Wofsy, J. M. Hoell, Jr., R. J. Bendura, J. W. Drewry, R. J. McNeal, D. Pierce, V. Rabine, and R. L. Snell, The Arctic Boundary Layer Expedition (ABLE) 3B: July-August 1990, *J. Geophys. Res.*, this issue (*a*).

Harriss, R. C., G. W. Sachse, J. E. Collins, L. Wade, R. W. Talbot, E. V. Browell, L. A. Barrie, K. B. Bartlett, and G. F. Hill, Carbon monoxide and methane over Canada: July-August 1990, *J. Geophys. Res.*, this issue (*b*).

Hegg, D. A., F. E. Radke, P. V. Hobbs, R. A. Rasmussen, and P. J. Riggan, Emissions of trace gases from some biomass fires, *J. Geophys. Res.*, *95*, 5669–5675, 1990.

Ingram, W. J., C. A. Wilson, and J. F. B. Mitchell, Modeling climate change: An assessment of sea ice and surface albedo feedbacks, *J. Geophys. Res.*, *94*, 8609–8622, 1989.

Iverson, T., On the atmospheric transport of pollution to the Arctic, *Geophys. Res. Lett.*, *11*, 457–460, 1984.

Jacob, D., et al., Summertime photochemistry in the Arctic troposphere, *J. Geophys. Res.*, *97*, 16,421–16,431, 1992.

Karentz, D., DNA repair mechanisms in Antarctic marine organisms, *Antarct. J. U.S.*, *13*, 114–115, 1988.

Keeling, C. D., A. F. Carter, and W. G. Mook, Seasonal, latitudinal and secular variations in the abundance and isotopic ratios of atmospheric CO_2, *J. Geophys. Res.*, *89*, 4615–4628, 1984.

Levine, J. S., Global biomass burning: Atmospheric, climatic, and biospheric implications, *Eos Trans. AGU*, *71*, 1075–1077, 1990.

Levine, J. S. (ed.), *Global Biomass Burning: Atmospheric, Climatic and Biospheric Implications*, MIT Press, Cambridge, Mass., 1991.

Levine, J. S., C. P. Rinsland, and G. M. Tennille, The photochemistry of methane and carbon monoxide in the troposphere in 1950 and 1985, *Nature*, *318*, 254–257, 1985.

Levy, H., II, Photochemistry of the lower troposphere, *Planet. Space Sci.*, *20*, 919–935, 1972.

Lightman, P., A. S. Kallend, A. R. W. Marsh, B. M. R. Jones, and S. A. Penkett, Seasonal variations of hydrocarbons in the free troposphere at mid-latitudes, *Tellus*, *42*(B), 408–422, 1990.

Logan, J. A., M. J. Prather, S. C. Wofsy, and M. B. McElroy, Tropospheric chemistry: A global perspective, *J. Geophys. Res.*, *86*, 7210–7254, 1981.

National Academy of Sciences (NAS), *Global Tropospheric Chemistry: A Plan for Action*, National Academy Press, Washington, D. C., 1984.

Prinn, R., et al., Global average concentration and trend for hydroxyl radicals reduced from ALE/GAGE trichloroethane (methyl chloroform) date for 1978–1990, *J. Geophys. Res.*, *97*, 2445–2461, 1992.

Radke, L. F., D. A. Hegg, P. V. Hobbs, J. D. Nance, J. H. Lyons, K. K. Laursen, R. E. Weiss, P. J. Riggan, and D. E. Ward, Particulate and trace gas emissions from large biomass fires in North America, in *Global Biomass Burning: Atmospheric, Climatic and Biospheric Implications*, edited by J. S. Levine, pp. 209–224, MIT Press, Cambridge, Mass., 1991.

Rahn, K. A., and R. J. McCaffrey, On the origin and transport of the winter Arctic aerosol, *Ann. New York Acad. Sci.*, *338*, 486–503, 1980.

Ramanathan, V., R. J. Cicerone, H. B. Singh, and J. T. Keihl, Trace gas trends and their potential role in climate change, *J. Geophys. Res.*, *90*, 5547–5566, 1985.

Rasmussen, R. A., and M. A. K. Khalil, Latitudinal distributions of trace gases in and above the boundary layer, *Chemosphere*, *11*, 227–235, 1982.

Rasmussen, R. A., M. A. K. Khalil, and R. J. Fox, Altitudinal and temporal variation of hydrocarbons and other gaseous tracers of Arctic haze, *Geophys. Res. Lett.*, *10*, 144–147, 1983.

Riley, J. L., Hudson Bay lowland floristic inventory, wetlands catalogue and conservation strategy, *Natur. Con. (Rev. Ecol. Syst.)*, *109*, 543–555, 1982.

Rinsland, C. P., and J. S. Levine, Free tropospheric carbon monoxide concentrations in 1950 and 1951 deduced from infrared total column amount measurements, *Nature*, *318*, 4522–4525, 1985.

Rinsland, C. P., and J. S. Levine, Identification and measurement of atmospheric ethane (C_2H_6) from a 1951 infrared solar spectrum, *Appl. Opt.*, *25*, 4522–4525, 1986.

Rinsland, C. P., J. S. Levine, and T. Miles, Concentration of methane in the troposphere deduced from 1950 infrared solar spectra, *Nature*, *318*, 245–249, 1985.

Rowland, F. S., and M. J. Molina, Chlorofluoromethanes in the environment, *Rev. Geophys.*, *13*, 1–35, 1975.

Rudolph, J., Two-dimensional distribution of light hydrocarbons: Results from the STRATOZ III experiment, *J. Geophys. Res.*, *93*, 8367–8377, 1988.

Rudolph, J., D. H. Ehhalt, and A. Tonnissen, Vertical profiles of ethane and propane, *J. Geophys. Res.*, *86*, 7267–7272, 1981.

Seiler, W., and P. J. Crutzen, Estimates of gross and net flux of carbon between the biosphere and atmosphere from biomass burning, *Clim. Change*, *2*, 226–247, 1980.

Shipham, M., S. Bachmeier, D. R. Cahoon, G. L. Gregory, B. E. Anderson, and E. V. Browell, A meteorological interpretation of the Arctic Boundary Layer Expedition (ABLE) 3B flight series, *J. Geophys. Res.*, this issue.

Singh, H. B., Reactive nitrogen in the troposphere, *Environ. Sci. Technol.*, *21*, 320–327, 1987.

Singh, H. B., and P. L. Hanst, Peroxyacetyl nitrate (PAN) in the unpolluted atmosphere: An important reservoir for nitrogen oxides, *Geophys. Res. Lett.*, *8*, 941–944, 1981.

Singh, H. B., and P. R. Zimmerman, Atmospheric distribution and sources of nonmethane hydrocarbons, in *Gaseous Pollutants: Characterization and Cycling*, edited by J. O. Nriagu, pp. 177–235, John Wiley, New York, 1992.

Singh, H. B., W. Viezee, and L. J. Salas, Measurements of selected C_2-C_5 hydrocarbons in the troposphere: Latitudinal, vertical, and temporal variations, *J. Geophys. Res.*, *93*, 15,861–15,878, 1988.

Singh, H. B., D. O'Hara, D. Herlth, J. D. Bradshaw, S. T. Sandholm, G. L. Gregory, G. W. Sachse, D. R. Blake, P. J. Crutzen, M. A. Kanakidou, Atmospheric measurements of PAN and other organic nitrates at high latitudes: Possible sources and sinks, *J. Geophys. Res.*, *97*, 16,511–16,522, 1992.

Singh, H. B., D. O'Hara, D. Herlth, W. Sachse, D. R. Blake, J. D. Bradshaw, M. Kanakidou, and P. J. Crutzen, Acetone in the atmosphere: Distribution, sources, and sinks, *J. Geophys. Res.*, this issue.

Smith, T. W., Jr., Summertime tropospheric nonmethane hydrocarbon and halocarbon concentrations over central and eastern Canada during ABLE 3B, Ph.D. dissertation, Univ. of Calif., Irvine, 1993.

Stith, J. L., L. F. Radke, and P. V. Hobbs, Particle emissions and the production of ozone and nitrogen oxides from the burning of forest slash, *Atmos. Environ.*, *15*, 73–82, 1981.

Stocks, B. J., The extent and impact of forest fires in northern circumpolar countries, in *Global Biomass Burning: Atmospheric, Climatic and Biospheric Implications*, edited by J. S. Levine, pp. 197–202, MIT Press, Cambridge, Mass., 1991.

Sze, N. D., Anthropogenic CO emissions: Implications for the atmospheric CO-OH-CH_4 cycle, *Science*, *195*, 673–675, 1977.

Tille, K. J. W., M. Savelsberg, and K. Bächmann, Airborne measurements of nonmethane hydrocarbons over western Europe: Vertical distributions, seasonal cycles of mixing ratios, and source strengths, *Atmos. Environ.*, *19*, 1751–1760, 1985.

Tyler, S. C., Chlorinated hydrocarbons in the troposphere, Ph.D. dissertation, Univ. of Calif., Irvine, 1983.

Wang, C. J.-L., Global concentrations of selected halocarbons, 1988–1992, Ph.D. dissertation, Univ. of Calif., Irvine, 1993.

Weiss, R. F., The temporal and spatial distribution of tropospheric nitrous oxide, *J. Geophys. Res.*, *86*, 7185–7195, 1981.

Wofsy, S. C., Interactions of CH_4 and CO in the Earth's atmosphere, *Am. Rev. Earth Planet. Sci.*, *4*, 441–469, 1976.

Wofsy, S. C., et al., Atmospheric chemistry in the Arctic and

subarctic: Influence of natural fires, industrial emissions, and stratospheric inputs, *J. Geophys. Res.*, *97*, 16,731–16,746, 1992.
Wofsy, S. C., et al., Factors influencing atmospheric composition over subarctic North America during summer, *J. Geophys. Res.*, this issue.
Zimmerman, P. R., J. P. Greenberg, and C. Westberg, Measurement of atmospheric hydrocarbon and biogenic emission fluxes in the Amazon boundary layer, *J. Geophys. Res.*, *93*, 1407–1416, 1988.

D. R. Blake, T. Y. Chen, F. S. Rowland, T. W. Smith, and W. J. Whipple, Department of Chemistry, University of California, Irvine, CA 92717.

(Received August 14, 1992; revised August 7, 1993; accepted September 10, 1993.)